Influence of the St John´s wort extract Ze117 and selected ingredients on membrane fluidity and phospholipid composition in rat C6 glioblastoma cells.

Dissertation

zur Erlangung des Doktorgrades (Dr. rer. nat.)
der Mathematisch-Naturwissenschaftlichen Fakultät
der Rheinischen Friedrich-Wilhelms-Universität Bonn

vorgelegt von

Nelli Keksel

aus

Druschba, Kasachstan

Bonn 2018

Angefertigt mit Genehmigung der Mathematisch-Naturwissenschaftlichen
Fakultät der Rheinischen Friedrich-Wilhelms-Universität Bonn.

1. Gutachter: Prof. Dr. Hanns Häberlein
2. Gutachter: Prof. Dr. Christoph Thiele

Tag der Promotion: 28.08.2018
Erscheinungsjahr: 2018

Summary

Chronic stress has been recognized to represent a key factor for the development of depression. Among others cortisol has been described to mediate an adaptive effect on plasma membrane fluidity which may affect signal transduction of membrane-bound receptors and contribute to pathophysiological changes leading to depression.

Membrane fluidity can be measured by fluorescence anisotropy using DPH (1,6-diphenyl-1,3,5-hexatriene) and TMA-DPH (1-(4-(trimethylamino)phenyl)-6-phenylhexa-1,3,5-triene). While chronic incubation (6-8 days) with terbutaline or dobutamine did not affect membrane fluidity of C6 cells, chronic exposure to cortisol dose-dependently decreased DPH and TMA-DPH fluorescence anisotropy, reflecting an increase in membrane fluidity. In contrast, cells pretreated with St. John's wort extract Ze117 showed increased DPH and TMA-DPH fluorescence anisotropy values, indicating a membrane rigidification effect which was mediated at least by the constituents hypericin, hyperforin, quercetin, amentoflavone and biapigenin. Rutin showed no effect. The tricyclic antidepressant desipramine (DMI) also showed to expose an adaptive decrease in membrane fluidity, however, only in the membrane core as measured by increased DPH fluorescence anisotropy. Chronic incubation with citalopram on the other side exposed no impact on membrane fluidity. Therefore it can be assumed that Ze117, and in part DMI, have a "normalizing" effect on the membrane fluidity of "stressed" cells.

Focusing on underlying lipidomic changes a decrease of the phosphatidylcholine to phosphatidylethanolamine (PC/PE) ratio was found in whole cell lipid extracts after chronic cortisol and Ze117 exposure which resulted at least in part from a decreased PC de-novo synthesis. In contrast to cortisol, which mediated a nonsignificant small decreased incorporation of choline-D9 into all main PC species under investigation, chronic Ze117 incubation selectively inhibited the synthesis of PC species bearing saturated or monounsaturated fatty acids.
Citalopram and DMI had no impact on the PC/PE ratio and the choline-D9 incorporation rate.

Zusammenfassung

Mittlerweile gilt es als erwiesen, dass dauerhafter Stress eine maßgebende Rolle bei der Entstehung von Depression spielt. Unter anderem wurde für Cortisol ein adaptiver Effekt auf die Membranfluidität nachgewiesen. Diese Veränderung der Membranfluidität dereguliert möglicherweise die Signaltransduktion membrangebundener Rezeptoren und bewirkt hierbei pathophysiologische Veränderungen, die zur Manifestierung einer Depression führen.

Die Membranfluidität kann unter anderem mittels DPH (1,6-diphenyl-1,3,5-hexatriene) und TMA-DPH (1-(4-(trimethylamino)phenyl)-6-phenylhexa-1,3,5-triene) Fluoreszenzanisotropie gemessen werden. Nach chronischer Inkubation (6-8 Tage) mit Terbutalin und Dobutamin wurden keine Veränderung in der Membranfluidität von C6 Zellen nachgewiesen. Nach chronischer Inkubation mit Cortisol jedoch wurde ein dosisabhängiger Abfall in der DPH sowie der TMA-DPH Fluoreszenzanisotropie gefunden und somit eine gesteigerte Membranfluidität. Gegensätzlich führte eine chronische Inkubation mit Ze117 im Vergleich zur Kontrolle zu einem dosisabhängigen Anstieg der DPH und TMA-DPH Fluoreszenzanisotropie. Dieser Effekt konnte unter anderem den Inhaltsstoffen Hypericin, Hyperforin, Amentoflavon, Biapigenin und Quercetin zugeschrieben werden. Das trizyklische Antidepressivum Desipramin (DMI) zeigte ebenfalls eine adaptive Versteifung der Plasmamembran, jedoch nur innerhalb des hydrophoben Membrankerns, da ein selektiver Anstieg der Fluoreszenzanisotropie nur unter Verwendung von DPH zu beobachten war. Citalopram zeigte keinen Einfluss. Daher könnte Ze117 und zum Teil auch DMI einen „normalisierenden“ Einfluss auf die Membranfluidität “gestresster“ Zellen haben.

Parallel ausgeführte Lipiduntersuchungen in C6 Ganzzell-Lipidextrakten zeigten eine Abnahme im Phosphatidylcholin zu Phosphatidylethanolamin (PC/PE) Verhältnis nach chronischer Behandlung mit Ze117 und Cortisol. Diese Effekte sind zumindest teilweise auf eine Abnahme der PC de-novo Biosynthese zurück zu führen. Hierbei wurde für Cortisol ein kleiner aber nicht signifikanter Abfall in der Choline-D9 Inkorporationsrate in allen hauptsächlich vorkommenden PC-Spezies festgestellt. Hingegen führte Ze117 zu einer

selektiven Inhibierung der Synthese von gesättigten und einfach ungesättigten Fettsäuren tragenden PC-Spezies. Citalopram und DMI hatten keinen Einfluss auf das PC/PE Verhältnis und die Choline-D9 Inkorporationsrate.

List of Abbreviations

$\parallel$	Parallel
$\perp$	Perpendicular
λ_{em}	Wavelength of emitted light
λ_{ex}	Wavelength of exited light
β_1-AR	β_1-adrenergic receptor
β_2-AR	β_2-adrenergic receptor
ACS	Acyl-CoA synthetase
BBB	Blood-brain barrier
Bkg	Background
C6	C6 rat glioblastoma
CCT	CTP:phosphocholine cytidylyltransferase
CK	Choline kinase
CoA	Coenzyme A
cPLA2	Cytosolic phospholipase A_2
CPT	Cholinephosphotransferase
D	Deuterium
DAG	Diacylglycerol
DHA	Docosahexaenoic acid
DMEM/F-12	Dulbecco`s modified Eagle medium
DMI	Desipramine
DMSO	Dimethyl sulfoxide
DPH	1,6-diphenyl-1,3,5-hexatriene
DSMZ	German collection of microorganisms and cell cultures
ECT	Electroconvulsive therapy
EDTA	Ethylenediaminetetraacetic acid
EPA	Eicosapentaenoic acid
ESI	Electrospray ionization
FBS	Fetal bovine serum
GPAT	Glycerol-3-phosphate acyltransferase
GPCR	G protein-coupled receptor
HBSS	Hank´s balanced salt solution

HPA	Hypothalamic-pituitary-adrenal
HPLC	High performance liquid chromatography
HPTLC	High performance thin layer chromatography
LPCAT	Lysophocholine acyltransferase
LPLAT	Lysophospholipid acyltransferase
m/z	Mass-to-charge ratio
MS	Mass spectrometry
MβCD	Methyl-β-cyclodextrin
PC	Phosphatidylcholine
PDL	Poly-D-lysine
PE	Phosphatidylethanolamine
PI	Phosphatidylinositol
PKC	Protein kinase C
PLA_2	Phospholipase A_2
PTSD	Posttraumatic stress disorder
PUFA	Polyunsaturated fatty acid
r	Anisotropy
R2	Coefficient of determination
RT	Room temperature
SEM	Standard error of the mean
SM	Sphingomyelin
SSRI	Selective serotonine reuptake inhibitor
TCA	Tricyclic antidepressant
TLC	Thin layer chromatography
TMA-DPH	1-(4-(trimethylamino)phenyl)-6-phenylhexa-1,3,5-triene
UV	Ultraviolet
v/v	Volume per volume
WHO	World Health Organisation
x g	Units of gravity

Content

1 Introduction

1.1 Depression and treatment approaches

Depressive disorders are dramatically disabling and potentially life-threatening diseases that are estimated to affect up to 20% of the population worldwide (*Berton & Nestler, 2006; Charney & Manji, 2004; DGPPN et al., 2015; Wong & Licinio, 2001*).

Therefore, depression belongs to the most frequent psychiatric disorders and represent a leading cause of disability, according to the WHO (*Reddy, 2010; Hay, 2017; Davis et al., 2017*).

For the treatment of depressive disorders psychotherapy, antidepressant medication, and in severe cases electroconvulsive therapy (ECT) are applied dependent on the individual assessed risk-benefit profile (*Fava & Kendler, 2000; DGPPN et al., 2015*). Standard antidepressant medication include for example selective serotonin reuptake inhibitors (SSRI), tricyclic antidepressants (TCA) and alternatively to synthetic antidepressants herbal medical products. Under these Hypericum perforatum (St John's Wort) dried extracts are the most common and are recommended and applied for the treatment of mild to moderate depression (*DGPPN et al., 2015; Ernst, 2007; Concerto et al., 2017*). Clinical meta-analysis demonstrated a similar effectiveness of Hypericum perforatum preparations compared to standard antidepressants, however with a much better adverse effect profile (*Whiskey et al., 2001; Ernst, 2007; Sarris, 2011*).

1.2 Depression and stress

Although the underlying pathology of depression remains to be completely understood, it is generally accepted that chronic stress and stressful life events (especially in early childhood) strongly predispose an individual to develop a clinical depression (*Faria et al., 2014; Charney & Manji, 2004; Hindmarch, 2001; Massart et al., 2012; Duman et al., 2016; Magalhães et al., 2017*). Chronic stress leads to a hyperactivation of the sympathetic nervous system and the hypothalamic-pituitary-adrenal (HPA) axis, resulting in increased circulation of catecholamines and glucocorticoids (e.g. cortisol) (*Chrousos, 2009; Gunnar &*

Quevedo, 2007). The HPA axis mediates and regulates prolonged stress response (*Weisbuch et al., 2009*) providing metabolic support by mobilizing glucose from energy stores by glycogen degradation (*Rabasa & Dickson, 2016*) and suppressing growth, maturation and the immune response (*van Bodegom et al., 2017; Kyrou & Tsigos, 2007*). Glucocorticoids induce stress adaption mainly by interaction with glucocorticoid receptors, which modulate gene expression (*Dindia et al., 2012; De Kloet et al., 2005; Tsigos & Chrousos, 2002; van Bodegom et al., 2017*). In contrast to catecholamines, which do not easily cross the blood-brain barrier (BBB), the brain represents the major target organ for glucocorticoids (*Gunnar & Quevedo, 2007*). Extreme or chronic stress exposure and subsequent continuous upregulation of glucocorticoids eventually induce adaptive changes which have health-damaging long-term consequences contributing to the psychopathology of multiple stress-related mental illnesses like depression and posttraumatic stress disorder (PTSD) (*Davis et al., 2017; Duman et al., 2016; Magalhães et al., 2017; Kyrou & Tsigos, 2007; van Bodegom et al., 2017*). Especially in the hippocampus chronically upregulated cortisol mediate deleterious changes in neuroplasticity, eventually leading to functionally disrupted negative-feedback mechanisms, which result in hyperactivity of the HPA axis *(Frodl & O`Keane, 2013; Lee et al., 2010; Andrade & Rao, 2010).*

1.3 Stress and membrane fluidity

Hypercortisolemia has been described to disturb monoaminergic systems in a manner similar as observed in depression (*De Kloet et al., 2005; Tafet & Bernardini, 2003*). This include among others a down regulation of ß-adrenergic receptors (*Fernstrom, 1994; Jakobs et al., 2013*) and the serotonin 1_A receptor (*Fernandes et al., 2017; Charney & Manji, 2004*). Beside changes in receptor density, changes in receptor activity have been described as well. These include for example an augmentation in serotonin 1_A receptor signaling (*Joca et al., 2007; Fernstrom, 1994*).

On the other side, chronic glucocorticoid exposure has also been demonstrated to modulate membrane properties. In this context a changed membrane fluidity has been examined by several chronic approaches applying cortisol and chemically similar glucocorticoids including hydrocorticosterone and

dexamethasone in human lymphocytes (*Tolentino et al., 1991*), HeLa cells (*Johnston & Melnykovych, 1980*), rat liver, and intestinal membranes (*Kapitulnik et al., 1986; Neu et al., 1986; Brasitus et al., 1987).*

Membrane fluidity refers to the molecular disorder and motion within the membrane bilayer (*Los & Murata, 2004*). A change in membrane fluidity has a modulatory impact on the lateral mobility and activity of membrane-bound receptors (*Los & Murata, 2004; Fajardo et al., 2011; Ohvo-Rekilä et al. 2002*). A direct cortisol induced alteration in membrane fluidity has for example been correlated to altered synaptosomal plasma membrane-associated Na^+, K^+-ATPase activity (*Deliconstantinos, 1985*). Such a direct cortisol-induced change in membrane fluidity may affect signaling pathways as shown for protein kinase-mediated phosphorylation, which modulates the activity status of membrane associated receptors (*Dindia et al, 2012*).

The lipid composition of membranes substantially influences physiochemical properties like membrane fluidity. In general, the cholesterol content, phospholipid composition and length and saturation degree of attached fatty acids represent modulators of the membrane fluidity (*Fajardo et al., 2011*).

Remarkably, chronic unpredictable stress has been identified to alter phospholipid profiles in the brain of depressed mice with increasing phosphatidylcholine (PC) and phosphatidylethanolamine (PE) levels and decreasing phosphatidylinositol (PI) level (*Faria et al, 2014*). A very similar chronic unpredicted stress protocol in rats examined rather brain-area specific changes with a significant increase in hippocampal PI and a decrease in PE in the prefrontal cortex of rats (*Oliveria et al., 2016*). Increased PC levels were also found in postmortem prefrontal cortex samples of bipolar disorder patients (*Schwarz et al, 2008*) as well as abnormalities in PI turnover with depression and bipolar disorders (*Farooqui et al., 2000*).

Epidemiological studies also revealed a reduced level of polyunsaturated omega-3 fatty acids (docosahexaenoic acid (DHA) and eicosapentaenoic acid (EPA)) in depressed patients (*Peet & Stokes, 2005; Logan, 2003; Fernandes et al., 2017*). DHA and to a lesser extend EPA are especially enriched in brain synaptic membranes and have a high impact on membrane fluidity and functional activity of membrane proteins (*Kidd, 2004; Kidd, 2007; Weiser et al.,*

2016; Dyall, 2015). And in fact EPA and DHA have been described to modulate ion channels (*Mischoulon & Rosenbaum, 2008; Kidd, 2004*), inhibit the protein kinase C (PKC) signal transduction enzyme complex (*Kidd, 2004*) and even modulate neurotransmitter signaling. For example EPA blocks the prostaglandin-mediated inhibition of serotonin release from presynaptic membranes, and DHA improves membrane embedded serotonin receptor accessibility (*Patrick & Ames, 2015*). Interestingly, DHA and EPA seem to inverse correlate with HPA axis activity in depressed patients *(Fernandes et al., 2017*).

In addition multiple investigations described a correlation between acute and chronic elevated glucocorticosteroid levels and increase in cholesterol content (*Floyd et al., 2007; Filburn 2000; Yehuda et al., 2000*), the precursor of steroid hormones like cortisol (*Yehuda et al., 2000*). On the other side a low concentration of cholesterol and high concentration of cortisol, was described in major depressed patients (*Jow et al., 2006; Papakostas et al., 2004*) and in suicide behavior (*Marcinko et al., 2005*). This depletion in cholesterol probably results from HPA axis hyperactivity and the correlating high demand in cortisol synthesis.

1.4 Aim and approach

Chronic stress represents a key factor for predisposing an individual to develop a clinical depression. Besides changes in receptor expression, cortisol seems to modulate membrane-associated signaling by alterations in membrane properties like fluidity.

The present work investigates the possible influence of antidepressant medication with Hypericum perforatum dried extract Ze117 compared to synthetic antidepressants and stress hormones on the plasma membrane fluidity in C6 cells. As the antidepressant effect of Hypericum perforatum extracts originate from various bioactive ingredients, single constituents were also tested for a contributing effect on membrane fluidity.

In order to proper distinguish between an adaptive and a direct membrane interacting effect on membrane fluidity, C6 cells were incubated for an acute (1h) and a chronic (6-8 days) period of time. Membrane fluidity was assessed by fluorescence anisotropy measurements applying DPH (1,6-diphenyl-1,3,5-hexatriene) and TMA-DPH (1-(4-(trimethylamino)phenyl)-6-phenylhexa-1,3,5-triene), which probe the dynamic behavior of the surrounding lipid microenvironment within different depths of the plasma membrane. Adaptive changes in membrane fluidity are further correlated to lipidomic changes. PC and PE represent the most prominent phospholipids within biological membranes, showing opposite effects on membrane fluidity. An increase in PC/PE ratio correlates with an enhanced membrane fluidity. Approaching thin layer chromatography (TLC) alterations in the PC/PE ratio within whole cell lipid extracts was examined and further investigated for underlying changes in PC biosynthesis. Incubation with deuterated choline (choline-D9), the starting compound of the PC de-novo biosynthesis pathway, and subsequent detection by mass analysis hereby allows identification of PC-species specific changes in time-dependent choline-D9 incorporation. Finally PC-species under investigation were characterized by their fatty acid moieties.

2 Materials and Methods

2.1 Materials

2.1.1 Chemicals and reagents

Desipramine hydrochloride, citalopram hydrobromide, dobutamine hydrochloride, quercetin, rutin hydrate, DPH (1,6-diphenyl-1,3,5-hexatriene), TMA-DPH (1-(4-(trimethylamino)phenyl)-6-phenylhexa-1,3,5-triene), choline chloride, choline chloride-trimethyl-d9 (choline-D9), methyl-β-cyclodextrin (MβCD), L-α-phosphatidylcholine, L-α-phosphatidylethanolamine and cortisol were purchased from Sigma (Taufkirchen, Germany).

The Hypericum perforatum extract Ze117 (batch-no. V803900) was supplied by Max Zeller Söhne AG (Romanshorn; Switzerland).

Amentoflavone, biapigenin, hyperforin and hypericin were supplied by HWI pharma services GmbH (Rülzheim, Germany). All reagents for cell culture were from Gibco by Thermo Fisher Scientific (Bremen, Germany).

2.2 Methods

2.2.1 High performance liquid chromatography

High performance liquid chromatography was performed applying the Agilent 1200 HPLC system (Agilent Technologies, Wilmington, DE, USA) equipped with a degasser (G1322A), a quaternary pump (G1311A), an autosampler (G1329A) and a photodiode array detector (G1315D). The analytical column employed was a reversed-phase Symmetry ™ C18 HPLC-column of 150 mm × 3.9 mm and 5 µm particle size (Waters Corporation, Milford, Massachusette, USA). The Hypericum perforatum dried extract Ze117 dissolved in 50% ethanol (EtOH) and ingredient standards dissolved in methanol (MeOH) were injected to the HPLC system programmed as described in Table 2.2.1. Detection was performed at 254 nm and 590 nm. Chromatograms were registered and evaluated using Agilent Chemstation Software version B.04.01. Identification of ingredients was carried out by comparison of UV spectra and retention times to reference substances.

Table 2.2.1: HPLC linear gradient program and mobile phase composition

time in min	**mobile phase A** acetonitrile/ H_2O/ 85% phosphoric acid (19:80:1 v/v/v)	**mobile phase B** acetonitrile/ MeOH/ 85% phosphoric acid (59:40:1 v/v/v)	**flow rate** (ml/min)
0	100 %	0 %	0.5
8	100 %	0 %	0.5
15	92.5 %	7.5 %	0.5
37	50 %	50 %	0.5
52	0 %	100 %	0.5
52.01	0 %	100 %	1
85	0 %	100 %	1

2.2.2 Cell culture

2.2.2.1 General cell culture

Rat glioblastoma (C6) cells obtained from the DSMZ (Leibniz Institute DSMZ-German Collection of Microorganisms and Cell Cultures GmbH, Braunschweig, Germany) were generally cultured in Dulbecco`s modified Eagle medium (DMEM/F-12), supplemented with 5 % fetal bovine serum (FBS), 2 mM L-glutamine, 100 units/ml penicillin and 100 µg/ml streptomycin. C6 cells were cultured in 10 cm culture dishes containing 10 ml culture medium at 37 °C in a humid atmosphere containing 5% CO_2. All steps of cell cultivation and processing were performed under sterile conditions using only prewarmed (37 °C) solutions/media and trypsinization solutions.

Cell passaging into the next generation was performed as soon as cell confluency reached 80-95 %. For this procedure the “spend” medium was sucked away and attached C6 cells were trypsinized with 3 ml trypsin/EDTA® solution. Incubation was performed at 37 °C, 5 % CO_2 until cells detached. Trypsin was inactivated by adding 10 ml of culture medium and rinsing the culture dish at least twice. The cell suspension was transferred into a 15 ml Falcon tube. Centrifugation at 1300 x g for 3 min at room temperature (RT) was performed and the supernatant was sucked away. The gained cell pellet was resuspended in 1 ml culture medium and cell seeding into the next generation was performed using an appropriate splitting ratio, usually 1:20. Cells are seeded into a new Petri dish containing fresh 10 ml cell culture medium. Using a splitting ratio of 1:20 results in the next generation of C6 cells to become confluent again after 4 days. The new generation is marked on the top of the Petri dish with an increasing passage number (PN = n + 1). Incubation at 37 °C and 5 % CO_2 followed until cells again become confluent. C6 cells with a passage number (PN) of max. 30 were used for cell culturing and experimental processing. Parallel to the general cell culture, the splitting procedure was also used to seed C6 cells in preparation to experimental approaches.

2.2.2.2 Cell culture under chronic incubation

Chronic incubation of C6 cells was performed for at least 6 days using cell culture medium enriched with defined concentrations of test substances under investigation (Table 2.2.2.2). To each series of chronic experiments a corresponding untreated control was prepared. Solvents were individually added to each condition and to the untreated control, to reach a uniform solvent concentration of max. 0.15% MeOH and 0.25% EtOH.

An initial splitting ratio of 1:20 causes C6 cells to become confluent again on the 4th day of chronic incubation. Since 0.025-0.05 mg/ml of Ze117 and 1 µM cortisol showed an inhibitory effect on cell proliferation, cell cultures under these conditions have been directly seeded in higher cell numbers using an initial splicing ratio of 1:15 for 0.05 mg/ml Ze117 and 1:17 for 0.025 mg/ml Ze117 and 1 µM cortisol.

Table 2.2.2.2: List of test substances and applied concentrations within chronic investigation

category	substance	stock solutions:	assay concentrations, chronic approach
stress hormons	**terbutaline**	1 mM in H_2O	1, 0.1 µM
	dobutamine	1 mM in MeOH	1, 0.1 µM
	cortisol	1 mM in MeOH	1, 0.1, 0.01 µM
antidepressants	**DMI**	1 mM in 50% EtOH	1 µM
	citalopram	1 mM in 50% EtOH	1 µM
Hypericum perforatum extract and bioactive ingredients	**Ze117**	10 mg/ml in 50%EtOH	0.05, 0.025, 0.01 mg/ml
	hypericin	0.1 mM MeOH	0.1, 0.01, 0.001 µM
	hyperforin	1 mM in MeOH	1, 0.1, 0.01 µM
	quercetin	1 mM in MeOH	1.5, 1, 0.5 µM
	rutin	2 mM in MeOH	1 µM
	biapigenin	1 mM in MeOH	1.5, 1, 0.5 µM
	amentoflavone	1 mM in MeOH	1.5, 1, 0.5 µM
control substance	**choline**	1 M in H_2O	10 mM

At the 4th day of incubation C6 cells are split again and either seeded to grow on glass cover slips in preparation to fluorescence anisotropy measurements (see section 2.2.3.1) or are again transferred into new Petri dishes filled with 10 ml of the corresponding incubation medium. Seeding into new Petri dishes was performed using the splitting ratio 1:10. However, the splitting ratio was also

adjusted to 1:7 for 1 µM cortisol and 0.025 mg/ml Ze117 or 1:5 for 0.05 mg/ml Ze117 in order for all conditions to reach uniform confluent cells on the 6th day.

Optionally, at the 5th day C6 cell were exposed for the last 24 h of incubation to 50 µM choline-D9 in preparation to the pulse-chase approach (see section 2.2.4.3.1).

At the 6th day of chronic incubation, the medium was sucked away and the cell culture dishes were placed on ice under non sterile conditions. 2 ml of ice cold water was added and C6 monolayer were harvested by cell scraping. The gained cell suspension was transferred to a 15 ml Falcon tube placed on ice. Centrifugation for 3 min at 1300 x g followed. The supernatant was sucked away and the cell pellet within the 15 ml Falcon tube was immediately placed back on ice for further lipid analysis or stored at -20°C.

The described chronic treatment procedures and all including variations in preparation to experimental membrane fluidity and lipid analysis is also presented in Figure 2.2.2.2.

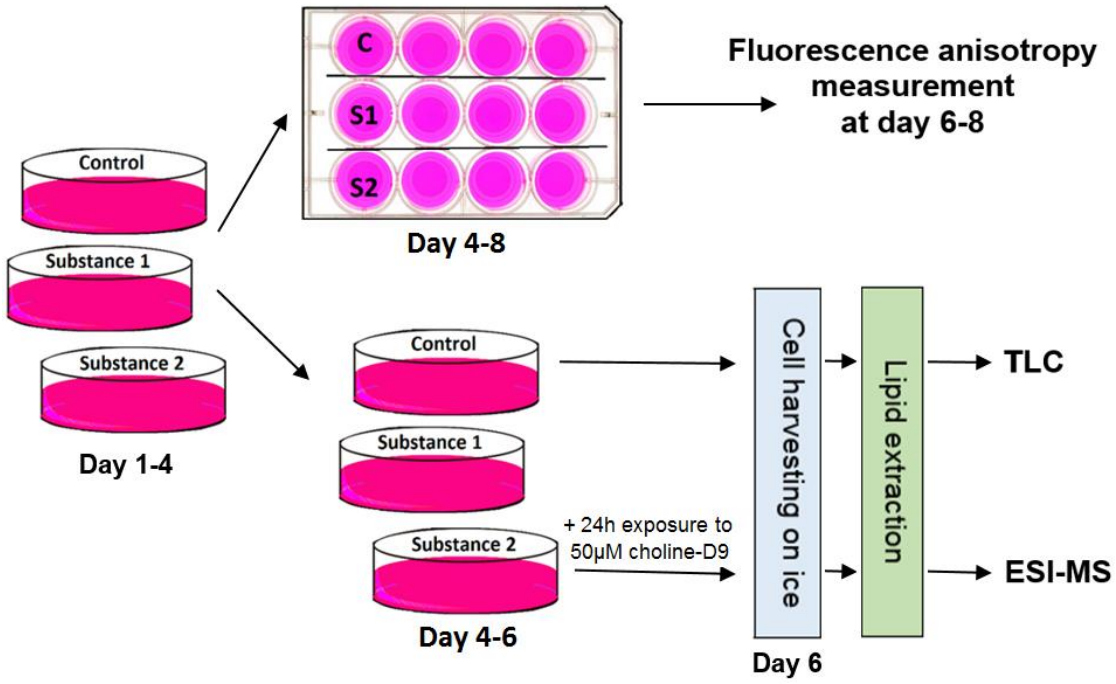

Figure 2.2.2.2: Experimental variations within cell culturing under chronic incubation in preparation to fluorescence anisotropy, TLC and ESI-MS approached in this work. C6 cells under chronic incubation were split at day 4 and seeded to grow on glass cover slips in 12-well plates in preparation to fluorescence anisotropy measurements at day 6-8. In preparation to lipid analysis via TLC and ESI-MS, C6 cells were seeded into new Petri dishes and were harvested at day 6 by cell scraping on ice, followed by lipid extraction. For the pulse-chase experiment applying ESI-MS analysis C6 cells were additionally exposed to 50 µM choline-D9 for the last 24 h of chronic incubation (6 days).

2.2.3 Membrane fluidity by fluorescence anisotropy measurements

2.2.3.1 C6 cells seeded on glass cover slips

In preparation to fluorescence anisotropy measurements, C6 cells were seeded in 12-well plates to grow on 13.5 x 13.5 mm glass cover slips, custom-build to exactly fit the inner diagonal plane of the cuvette.

C6 cells under chronic treatment conditions usually at the 4th day, or C6 cells under regular cell culture conditions for acute measurements were trypsinized by the usual procedure. In order for all cell samples to reach an appropriate and uniform confluency at the experimental day, individual cell concentration from each cell suspension was determined. The cell pellet resuspended in 1 ml cell culture medium was further diluted 1:10 and applied to a Neubauer counting chamber. The counting chamber was placed under a microscope and the cell concentration was determined according to Figure 2.2.3.1.

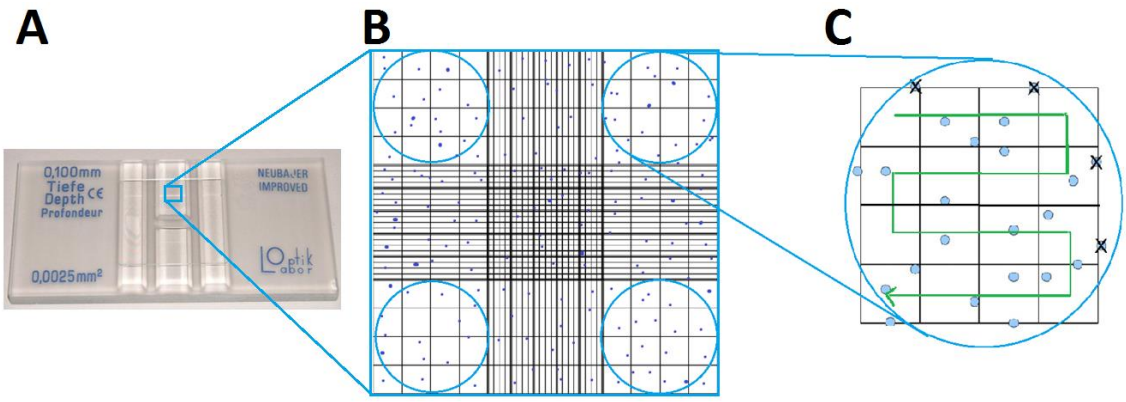

Figure 2.2.3.1: Cell concentration determination via Neubauer counting chamber. (A) One side (or both) of the Neubauer counting chamber is filled with the cell suspension of unknown cell concentration. A defined volume is sucked into the space between counting chamber and cover glass. (B) The microscopic view allows the visualization of 4 big squares, each containing 4 x 4 smaller squares (C), which is counted for the number of residing cells. The green arrow describes the direction of counting including all cells left and on the bottom, while excluding all cells bordering on the top and right to the large square. Finally the cell concentration is calculated using the following formula:

$$\frac{cells}{ml} = \frac{\text{n (counted cells)}\ x\ 10.000}{Number\ of\ squares\ x\ dilution\ factor} \qquad \text{(equation 1)}$$

The determined cell concentration allowed the uniform seeding of C6 cells into 12-well plates, with each well filled with a 13.5 x 13.5 mm glass cover slip and 1 ml of the corresponding incubation media. It is to be noted, that cells under chronic incubation with 0.025-0.05 mg/ml Ze117 were for reasons of better cell adherence seeded on poly-D-lysine (PDL) coated glass cover slips (see the following section). In general 70 000 cells/well were seeded for additional 2 days of incubation. For additional 3 and 4 days of incubation 30 000 and 10 000 cells/well were seeded, respectively. Cells under chronic incubation with higher concentrations of cortisol or Ze117 were seeded using cell numbers increased by 15% for 1 µM cortisol and 0.025 mg/ml Ze117 and 30% for 0.05 mg/ml Ze117.

2.2.3.2 PDL-coating of glass cover slips

For chronic incubation with Ze117 concentrations of 0.025 mg/ml and 0.05 mg/ml and their corresponding controls, C6 cells were seeded on poly-D-lysine (PDL) coated glass cover slips in 12-well plates. A stock solution of 100 x PDL (10 mg/ml in PBS) was diluted 1:100 to reach a final concentration of 1 x PDL. One ml of this solution was transferred to each well and incubated either for at least 1 h at 37°C or overnight at 4°C. Afterwards, each well was washed with PBS and the empty 12-well plates were dried for about 30 min at 37°C, ready for cell seeding as described above/in the previous section.

2.2.3.3 Acute exposure of adherent C6 cells before fluorescence anisotropy measurements

Fluorescence anisotropy measurements after acute exposure of C6 cells to substances under chronic investigation were performed in addition. For this purpose C6 cells under general cell culture conditions grown on glass cover slips were just prior to the measurement procedure transferred to a new 12-well plate and incubated for 1 h in 1 ml of the corresponding incubation medium. In detail those incubation media contained either 1 µM cortisol, terbutaline, dobutamine, DMI, citalopram, hyperforin, rutin or 1.5 µM quercetin, amentoflavone, biapigenin or 0.05 mg/ml Ze117. Afterwards the cover slip was washed 3 times in Hank´s

balanced salt solution without phenol red (HBSS - phenol red), ready for background (Bkg) determination for the fluorescence anisotropy measurement procedure (see section 2.2.3.5).

2.2.3.4 Cholesterol depletion in adherent C6 cells before fluorescence anisotropy measurement

Cholesterol depletion was performed by transfer and incubation of the cell monolayer grown on glass cover slips into a new well, filled with 1 ml 10 mM methyl-β-cyclodextrin (MβCD) in serum-free cell culture medium for 30 min at 37°C. The corresponding control cell monolayer of identical seeding procedure and confluency was in parallel also incubated with serum-free culture medium (without MβCD). Afterwards the cover slips were washed once in serum-free cell culture medium followed by washing 3 times in HBSS (- phenol red), ready for background (Bkg) determination for the fluorescence anisotropy measurement procedure (see section fluorescence anisotropy measurement).

2.2.3.5 Fluorescence anisotropy measurements on adherent cells grown on glass cover slips

Steady-state fluorescence anisotropy measurements (L-configuration) were performed using the LS 55 fluorescence spectrometer (Perkin-Elmer, Rodgau, Germany) equipped with a circulation thermostat connected to the cell sample holder allowing constant 37°C during measurements. The sample holder was rotated to adjust the cell monolayer within the cuvette to a 30° angle relative to the incident light beam, if not otherwise stated. Within the sample holder a 7 mm plastic piece was inserted, resulting in a higher stand of the cuvette and the light beam to toughly pass through the monolayer. The emission polarizer was set vertical and the absorption polarizer was set vertical or horizontal to allow intensity measurements of polarized light signals parallel ($_{II}$) by vertical and vertical (vv) and perpendicular ($_{\perp}$) by vertical and horizontal (vh) settings (Figure 2.2.3.5). For DPH and TMA-DPH these intensities were determined at λ_{ex}: 360 nm (slit 5 nm) and λ_{em}: 430 nm (slit 10 nm).

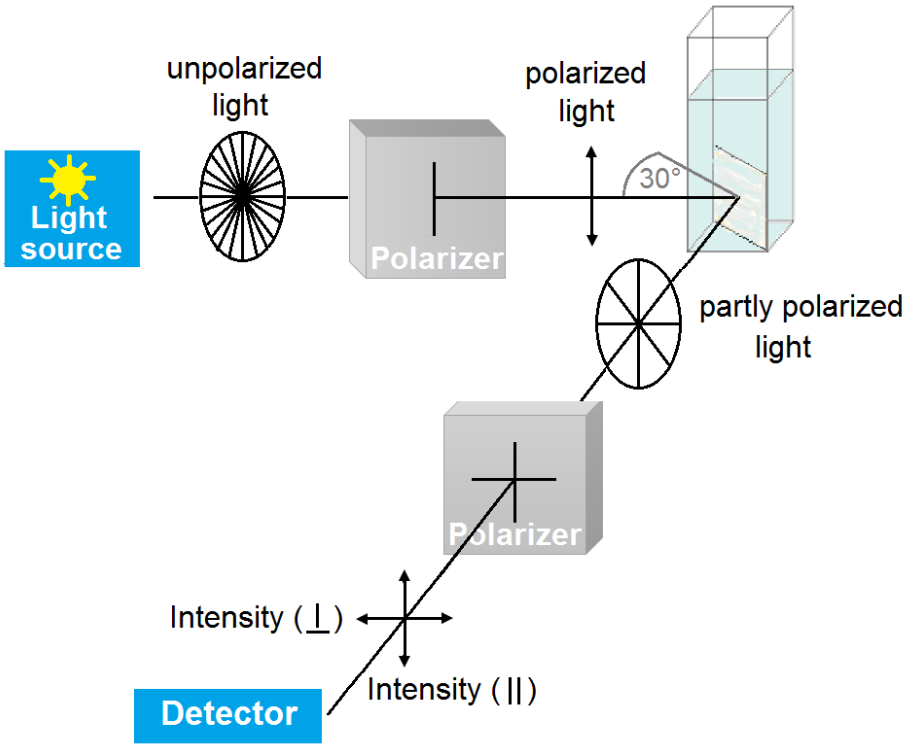

Figure 2.2.3.5: Principle of fluorescence anisotropy experimental setup. A light beam was polarized by a polarizer before reaching the cell monolayer (grown on glass cover slip) with an incident angle of 30°, if not other stated. This results in polarized emission of the excided-state fluorophores (DPH and TMA-DPH) along a preferential axis. With increasing rotational mobility during the absorption transition moment the emitted light was stronger distributed within different polarization planes (Intensity II and ⊥) resulting in a decreased anisotropy value.

Each monolayer grown on glass cover slips was prior to the labeling procedure washed 3 times with HBSS (- phenol red) and placed into a cuvette filled with 2 ml HBSS (- phenol red) and the individual cell background (Bkg) intensities parallel and perpendicular to the initial polarization were determined.
Labeling was performed by incubation of the cell monolayer with 90 µM DPH or 30 µM TMA-DPH in HBSS (- phenol red) for 30 min at 37°C. Afterwards cover slips were washed 3 times with HBSS (- phenol red) and placed again into the cuvette containing 2 ml of HBSS (- phenol red).

Table 2.2.3.5: Stock and working concentration of DPH and TMA-DPH.

	stock solution	labeling concentration
TMA-DPH	5 mM in EtOH	30 µM
DPH	10 mM in DMSO	90 µM

Within the following 30 min up to 7 individual fluorescence anisotropy measurements were performed, measuring intensities vv and vh. The measured intensities were corrected by subtracting the Bkg signals vv and vh from the measured intensity vv and vh and fluorescence anisotropy (r) was calculated using the formula below (*Chen et al., 1999*);

$$Anisotropy\ r = \frac{I\,vv - Gf \cdot I\,vh}{I\,vv + 2 \cdot Gf \cdot I\,vh} \quad \text{(equation 2)}$$

I vv=measured I vv – Bkg vv
I vh= measured Ivh – Bkg vh

$$Gf = \frac{I\,hv}{I\,hh} \quad \text{(equation 3)}$$

The grating factor (Gf) is determined previously to the anisotropy measurement and represents the correcting factor to compensate for the polarization bias of the instrumental polarization. Own measurements revealed a Gf of 1 and therefore it was neglected.

Each condition is measured in duplicates (2 samples of identical incubation condition) and finally normalized to the mean of the control (see section 2.2.5).

2.2.4 Phospholipid analysis

2.2.4.1 Lipid extraction

Falcon tubes containing cell pellets, harvested after chronic incubation, were placed on ice. The cell pellets were resolved in 0.5 ml ice cold distilled water and lysed by being forced at least 30 times through a 20 G cannula using a syringe. The whole cell homogenate was transferred into a small glass tube filled with 3 ml of a $CHCl_3$/MeOH solution (2:1, v/v) and a small stirring bar. The glass tubes were hermetical closed, proper vortexed and placed into a water bath at 60 °C and magnetic stirring for 4 h. Afterwards 1 ml of MeOH were added, receiving a $CHCl_3$/MeOH ratio of 1:1 (v/v). The tubes were again proper closed, vortexed and placed for additional 3.5 h under magnetic stirring in the 60 °C heated water bath. Finally, the solution was filtered through a glass wool plugged Pasteur pipette to separate the solution from precipitated proteins/non-lipid contaminants.

The collected lipid solution was concentrated by placing the open glass tubes into a 50 °C heated water bath under a gentle N_2-stream.

After ~ 1.5 h the solvent has completely removed and the dried lipid fraction was subsequently resolved in 200 µl $CHCl_3$/MeOH (1:1, v/v) for TLC analysis (see section below) or 100 µl of a isopropanol/hexane/100 mM ammonium formate mixture (50:40:10, v/v/v) or a $CHCl_3$/MeOH mixture (1:2, v/v) containing 5 mM ammonium acetate or ammonium chloride.

2.2.4.2 High performance thin layer chromatography of lipid extracts.

High performance thin layer chromatography (HPTLC) silica gel plates (20 x 10 x 0.2 cm) were just prior to experimental performance removed from the manufacturer´s storage box and conditioned for 5 min at 180°C. Each plate was loaded with a PE (0.25-1.5 µg) and PC (0.5-3 µg) standard, test samples and corresponding controls, all dissolved in $CHCl_3$/MeOH (1:1, v/v). Samples were spotted manually as 5 mm bands on HPTLC plates, keeping a spacing of 10 mm between samples and 15 mm margin from the bottom and the side edges of the plate.

TLC developing chamber (22 x 22 x 10.5 cm) was prepared, containing 94 ml freshly prepared mobile phase $CHCl_3$/MeOH/H_2O (65:25:4 (v/v/v)) and chromatography filter paper.

The TLC developing chamber was closed and allowed to saturate for about 1 h, until the solvent has run the entire height of the chromatography filter paper.

Afterwards up to 3 loaded HPTLC plates were placed into the camber. The camber was kept close again and within approximately 20 min HPTLC plates were socked with the mobile phase up to about 1 cm below the top. The plates were removed from the TLC chamber and air-dried, followed by being shortly immerged into a TLC detection immersion bath containing 10% copper (II) sulfate as detection reagent. HPTLC plates were dried using an air-blower until plates appear in a uniform light blue staining. The dried TLC plates were developed at 180°C for about 5-10 min until proper visualization of PE and PC bands.

Digital images of the developed TLC plates were generated and densitometrically analyzed using the Aida Image Analyzer software version 450 (Raytest,

Straubenhardt, Germany) under the inverted quantum level parameter. For each plate the detection area of densitometric determination was preset to an adjusted shape and size for PE and PC, respectively, enabling to fit these bands individually**.** This preset detection region was also applied to determine the corresponding background (Bkg) next to individual PE and PC bands. From each determined lipid signal the corresponding Bkg was subtracted, leaving the pure lipid signal. The resulting calibration curves (plotting µg vs. signal intensity) were applied for PE and PC quantification if an accuracy of $R^2 \geq 0.96$ was reached. The calculated µg-values of the PC and PE fractions from each sample were set into ratio (PC/PE) and are presented as relative change compared to the control PC/PE ratio.

2.2.4.3 Pulse-chase of phosphatidylcholine de-novo synthesis

2.2.4.3.1 Pulsing chronic incubated C6 cells with choline-D9 in preparation to ESI-MS

C6 cells under general cell culture conditions or C6 cells at the 5th day of chronic treatment conditions (see section 2.2.2.2) were 24 h before cell harvesting exposed to 50 µM choline-D9 (Figure 2.2.4.3).

For this purpose the spend medium was sucked away and 10 ml of new incubation medium of individual incubation conditions enriched with 50 µM choline-D9 was carefully added. After 24 h of incubation all reactions were stopped by harvesting C6 cells by scraping on ice. Lipids were extracted and dissolved in 100 µl isopropanol/hexane/100 mM ammonium formate mixture (50:40:10, v/v/v) as described previously (see section 2.2.4.1). The gained lipid extract was further diluted 1:20, ready for direct infusion ESI-MS analysis of choline-D9 incorporation into PC, as described below.

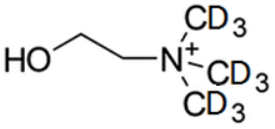

Figure 2.2.4.3.1: Chemical structure of choline-D9. The abbreviation D describes deuterium, the stable ^{2}H isotope (heavy hydrogen).

2.2.4.3.2 Chasing choline-D9 incorporation into PC via mass spectrometry

Detection of choline-D9 incorporation into individual PC species was performed on a HCT Ultra ion trap mass spectrometer (Bruker Daltonics, Bremen, Germany) equipped with an ESI ion source. The samples were loaded into a clean 250 µl Hamilton syringe and injected to the instrument with a continuous flow of 5 µl/min using the KDS 100 legacy syringe pump (KD Scientific, Boston, MA, USA).

Parameters of the MS instrument were as follows: positive mode, nebulizer pressure 16 psi; dry gas flow 7 l/min; dry gas temperature 300 °C; mass range 100-1000 m/z; scan speed 8.100 m/z per second. MS scans were recorded for 1 min. The gained sum MS spectra were analyzed using the DataAnalysis (Bruker Daltonics) software.

PC species and their deuterated derivatives were detected, exposing a mass-to-charge (m/z) difference of 9. Their identities as PC lipids were undoubtedly proven

by +MS2 mediated neutral loss of the head group (phosphocholine -183 m/z or phosphocholine-D9 -192 m/z) and the loss of trimethylamine (-59 m/z) or trimethylamine-D9 (-68 m/z) from the parent ion (Figure 2.2.4.3.2).

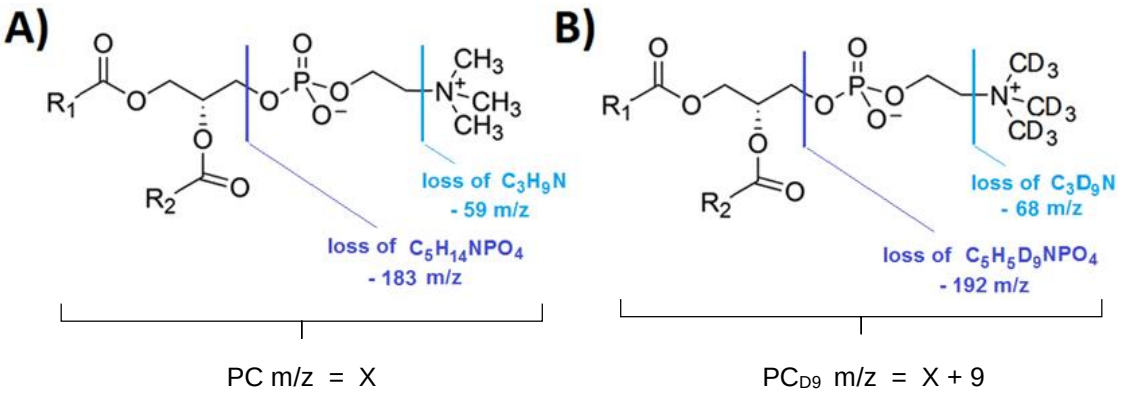

Figure 2.2.4.3.2: Identification principle of PC-pairs by positive mode mass analysis. Natural occurring PC species (A) and their deuterated derivatives (B) result from choline and choline-D9 incorporation via the de-novo biosynthesis pathway, respectively. The detectable mass shift of + 9 m/z results from the 3 deuterated methyl groups of choline-D9 incorporated into PC. The identities of PC lipids were proven within +MS2 by forming identical DAG-like products by the loss of phosphocholine (with m/z = 183) or phosphocholine-D9 (with m/z = 192). The loss of trimethylamine (with m/z = 59) or trimethylamine-D9 (with m/z = 68) from the parent ion is also examined.

For each sample, signal intensities of the most prominent PC species and their deuterated derivatives, were determined. Finally, the percentage amount of choline-D9 incorporation into each PC-species under investigation was calculated, applying the formula below;

$$\textit{Species dependent choline-D9 incorporation in \%} = \frac{I_{PC_{D9}} \times 100}{I_{PC_{D9}} + I_{PC}} \qquad \textit{(equation 4)}$$

I_{PC} = *Signal intensity of natural occurring PC species*

$I_{PC_{D9}}$ = *Signal intensity of corresponding deuterated PC species*

2.2.4.3.3 PC species identification via negative mode MS3

PC species of interest were further characterized by their fatty acid moiety combination via negative mode fragmentation. For this purpose lipid extracts (derived from C6 cells not exposed to choline-D9) were dissolved in 100 µl of a CHCl3/MeOH mixture (1:2, v/v) supplemented with 5 mM ammonium acetate or ammonium chloride, allowing negative mode observation of anionic PC adducts. Just prior to the measurement samples were further diluted 1:100 and analyzed for reasons of higher resolution with the TriVersa Nanomate chip-based electrospray device (Advion Biosciences, Ithaca, USA) coupled to the ultrahigh resolution LTQ Orbitrap Velos mass spectrometer (Thermo Fisher Scientific, Bremen, Germany). The instrument was controlled for data collection by the Xcalibur software version 2.2 (Thermo Fisher Scientific). Ionization voltage and gas (nitrogen) pressure were set to 1.6 kV and 0.3 psi, respectively. Within the negative full scan modus PC species were detected as $[M+CH_3COO]^-$ or $[M+Cl]^-$ adducts over a mass range of m/z = 700-900. Each PC species was isolated within an individual small m/z range window, followed by MS2 fragmentation in the ion trap under collision induced dissociation (CID) set to 35-40%. The gained $[M-CH_3]^-$ fragment was further isolated and fragmented leaving the final fatty acid products (Figure 2.2.4.3.3). The identity of the examined fatty acid products was determined by comparison to online data base (http://www.byrdwell.com/PhosphatidylCholine/FattyAcids.htm).

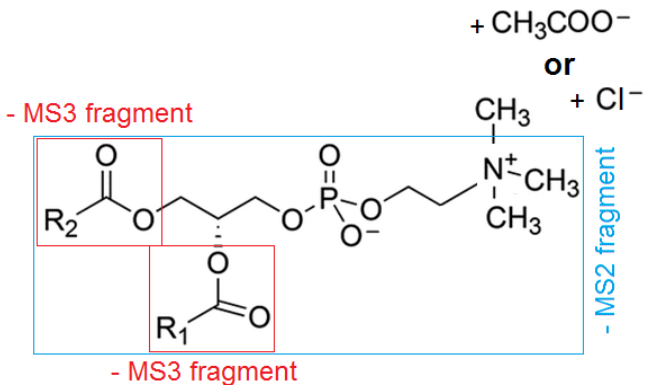

Figure 2.2.4.3.3: Identification principle of PC fatty acid moieties by negative mode mass analysis. PC is detected within the negative mode as anionic chloride $[M+Cl]^-$ or acetate $[M+CH_3COO]^-$ adduct. PC adduct was fragmented by –MS2 resulting in a $[M-CH_3]^-$ product. Following fragmentation of this $[M-CH_3]^-$ product by –MS3 leaves free fatty acid products. The sn-2 fatty acid product $[R_2COO]^-$ is distinguished from the sn-1 fatty acid product $[R_1COO]^-$ due to it appears with a higher abundancy within the -MS3 spectrum.

2.2.5 Result processing and statistics

Raw data were processed by Excel (Microsoft office 2013, Redmond, WA, USA). Results of fluorescence anisotropy measurements and PC/PE ratio assessments via TLC are presented as relative change compared to the control. Normalization was achieved by setting the mean value of the controls (MVc) from each independent experiment to 1. All associated measured values of control and test substances were set into relation to this MVc. Results of at least 3 independent experiments were pooled, with the exception of obvious outliner, and presented as *mean* and the *standard error of the mean* (SEM).

Outliner are defined for fluorescence anisotropy experiments by a deviation of ≥ 0.10 and ≥ 0.15 from the individual mean of each group for chronic and acute measurements, respectively.

Within TLC experiments for PC/PE ratio assessment only results generated by a calibration curve fitting linear range accuracy of $R^2 \geq 0.96$ were pooled.

Diagrams are generated using Prism V.6 software (GraphPad, La Jolla, CA, USA).

For statistical analysis the unpaired t-test was performed using the Prism V.6 software (GraphPad). Results significantly different from their corresponding control groups are marked by * $p \leq 0.05$, ** $p \leq 0.01$, *** $p \leq 0.001$.

3 Results

3.1 HPLC analysis of Ze117

The applied Hypericum perforatum dried extract Ze117 was characterized for the presence of relevant ingredients applying HPLC analysis. As presented in Figure 3.1 the applied Ze117 extract was identified to be rich in flavonoids including rutin, hyperoside, quercitrin, isoquercetin, quercetin, biapigenin, the phloroglucinol hyperforin, and the naphthodianthrones hypericin and pseudohypericin. Amentoflavone represents a minor constituent. Rutin, quercetin, biapigenin, amentoflavone, hyperforin and hypericin are presented in addition with chemical structure as these substances become relevant within following fluorescence anisotropy measurements.

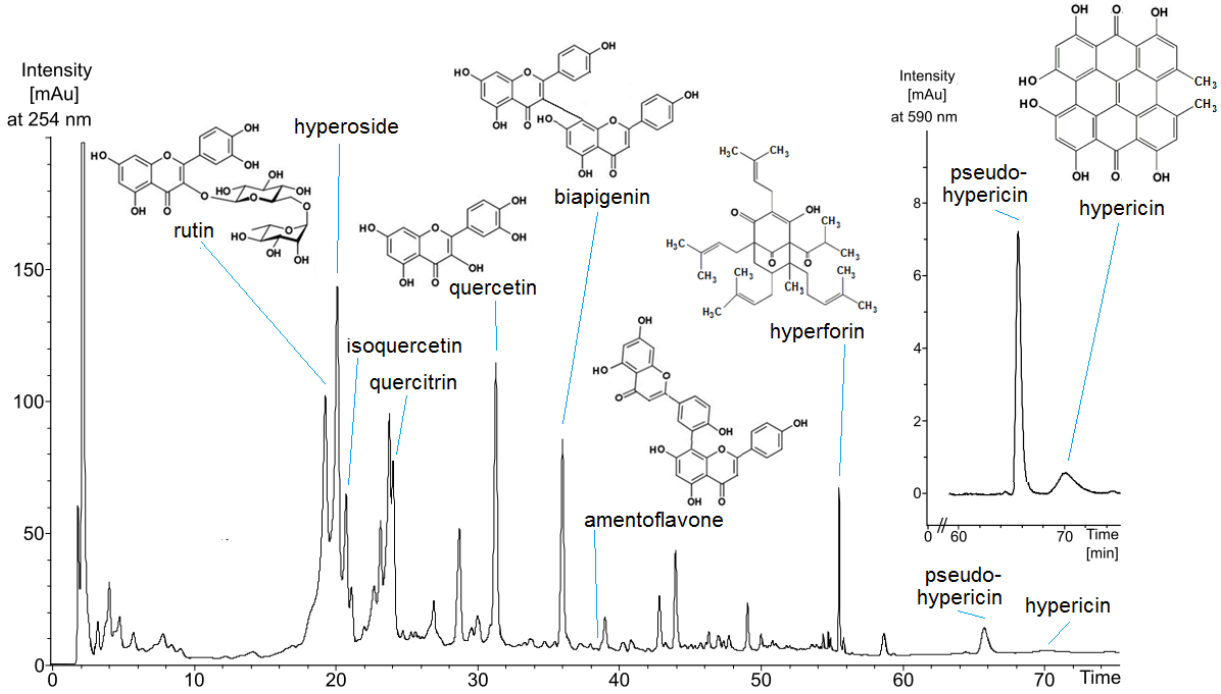

Figure 3.1: HPLC chromatogram of Ze117.

3.2 Fluorescence anisotropy

3.2.1 Evaluation of fluorescence anisotropy measurements

Within this study, changes of the plasma membrane fluidity of C6 cells were assessed by fluorescence anisotropy measurements. For this purpose DPH (1,6-diphenyl-1,3,5-hexatriene) and TMA-DPH (1-(4-(trimethylamino)phenyl)-6-phenylhexa-1,3,5-triene) were applied probing different plasma membrane depths.

Fluorescence anisotropy measurements, usually performed in cell suspensions, were performed on adherent C6 cell monolayers grown on glass cover slips keeping cells in their naturally adherent form. In comparison to the regular described light angle of 45° relative to the cell monolayer (referred to as the "magic angle") measurements performed at an incident light angle of 30° effectively minimized the background signal (Bkg) and led to more stable and reliable anisotropy measurements, as presented for TMA-DPH (Figure 3.2.1-1).

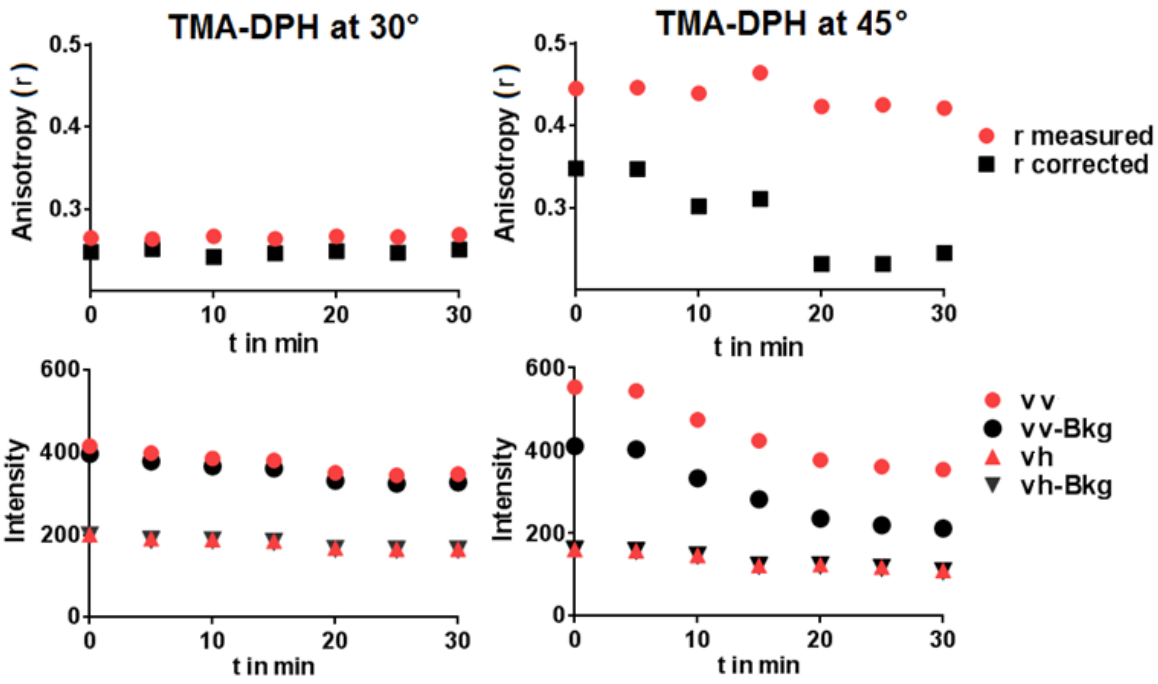

Figure 3.2.1-1: Changes in fluorescence anisotropy (r) and corresponding intensity values over time measured by TMA-DPH (30 µM, 30 min) in adherent C6 cells exposed to an incident light angle of 30° or 45° relative to the cell monolayer. (Upper panel) Anisotropy values are presented as the measured and the corrected anisotropy values (determined by Bkg subtraction). **(Lower panel)** The corresponding intensities measured at vertical/vertical (vv) and vertical/horizontal (vh) polarization settings are presented as measured and corrected values (after Bkg subtraction).

Within this experimental setup applying an incident light angle of 30° a labeling concentration of 30 µM TMA-DPH and 90 µM DPH incubated for 30 min at 37 °C was found to reach suitable intensities (after Bkg subtraction) for reliable anisotropy calculation. The low quantum of DPH compared to TMA-DPH, makes DPH more susceptible to signal fluctuations and Bkg noise interferences. This problematic situation could however be compensated by applying a 3-fold increased DPH concentration compared to TMA-DPH.

A typical DPH and TMA-DPH fluorescence anisotropy and intensity profile is presented in Figure 3.2.1-2. Although signal intensities showed to increase for DPH while TMA-DPH signal intensities decrease with passing time, a stable fluorescence anisotropy profile after Bkg subtraction (r corrected) was obtained over a time range of at least 60 min.

By this experimental approach we reached absolute DPH fluorescence anisotropy values of r = 0.17 - 0.25 and absolute TMA-DPH values of r = 0.24 - 0.32 in adherent C6 cells.

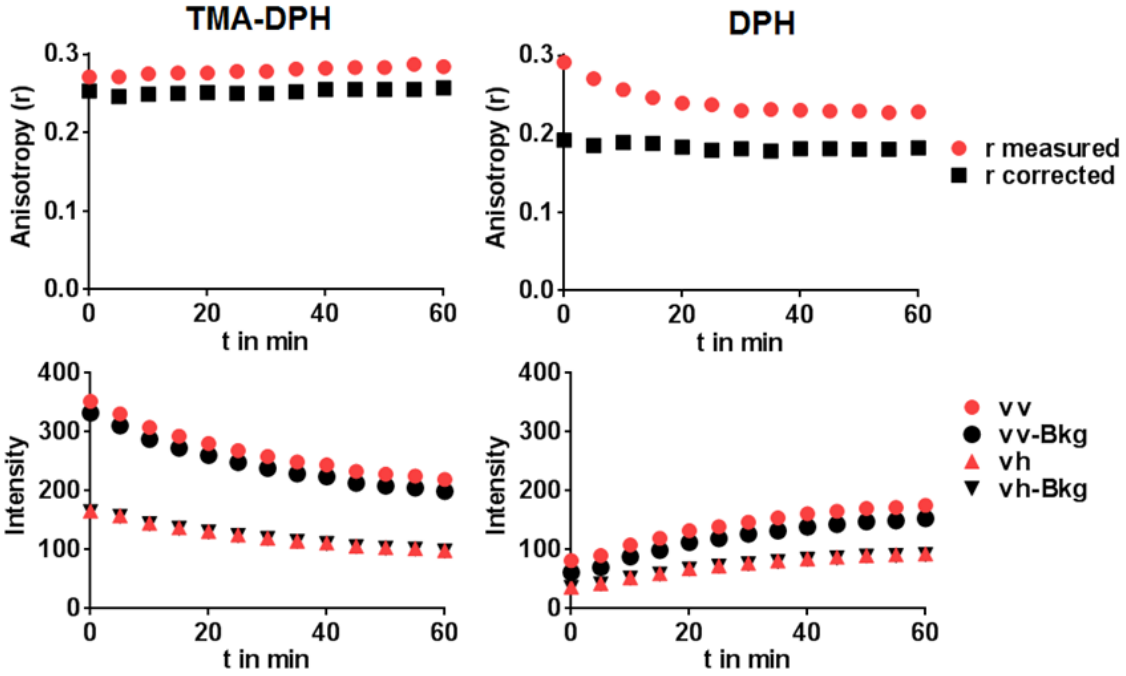

Figure 3.2.1-2: Typical time-dependent DPH and TMA-DPH fluorescence anisotropy (r) and intensity profile in adherent C6 cells, measured at a light angel of 30°. (Upper panel) Fluorescence anisotropy profile of DPH and TMA-DPH presented as measured and corrected (after Bkg substraction) anisotropy value. **(Lower panel)** The corresponding intensities measured at vertical/vertical (vv) and vertical/horizontal (vh) polarization settings are presented as measured and corrected values (after Bkg subtraction).

By quantitative manipulation of membrane components that are known to achieve fluidity changes in a measureable way, the validity of the experimental setup can be evaluated. The significance of DPH and TMA-DPH fluorescence anisotropy changes as indicator of membrane fluidity alterations, was evaluated both by cholesterol depletion using methyl-β cyclodextrine (MβCD) and by increasing the phosphatidylcholine (PC) content by exposing C6 cells chronically (6 days) to an excess of choline (Figure 3.2.1-3 and Table 3.2.1).

Cholesterol depletion, performed by incubation of C6 cells for 30 min at 37°C with 10 mM MβCD, mediated significantly reduced DPH and TMA-DPH fluorescence anisotropy values, compared to the control. Under MβCD treatment DPH reached a stronger reduction to 0.815 ± 0.043**, compared to TMA-DPH with 0.933 ± 0.008***.

After chronic treatment (6 days) of C6 cells with 10 mM choline, we found a significant reduction of TMA-DPH fluorescence anisotropy values to 0.968 ± 0.007** accompanied by the absence of an significant effect on DPH fluorescence anisotropy (Figure 3.2.1-3).

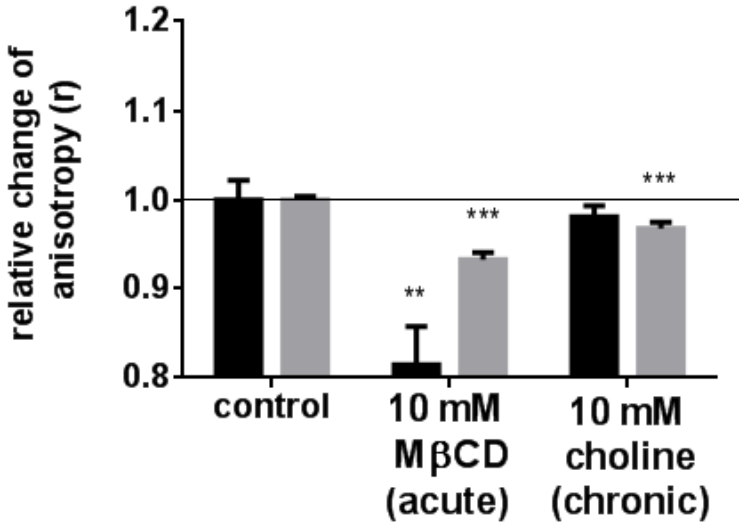

Figure 3.2.1-3: Relative change in DPH (■) and TMA-DPH (■) fluorescence anisotropy in adherent C6 cells after cholesterol depletion and PC enrichment. Cholesterol depletion was performed by incubation with 10 mM MßCD for 30 min. Enrichment of the PC content was performed by chronic incubation (6 days) with 10 mM choline. Results are presented as mean ± SEM. Marked values ** $p \leq 0.01$ and *** $p \leq 0.001$ are significantly different from their corresponding controls, determined by the unpaired t-test. For corresponding values see Table 3.2.1.

Table 3.2.1: Corresponding values to Figure 3.2.1-3. Relative changes in DPH and TMA-DPH fluorescence anisotropy of adherent C6 cells chronically exposed to 10 mM choline for 6 days or 10 mM MßCD for 30 min. Marked values ** p ≤ 0.01 and *** p ≤ 0.001 are significantly different from their corresponding controls, determined by the unpaired t-test.

		mean ± SEM	n-value of samples	n-value of independent experiments
DPH	control	1.000 ± 0.022	13	9
	10 mM MßCD	0.815 ± 0.043**	3	3
	10 mM choline	0.981 ± 0.012	10	6
TMA-DPH	control	1.000 ± 0.004	21	10
	10 mM MßCD	0.933 ± 0.008***	9	4
	10 mM choline	0.968 ± 0.007**	12	6

3.2.2 Chronic incubation of C6 cells

3.2.2.1 Stress hormones

Since depression is strongly correlated to chronic stress, C6 cells were chronically (6-8 days) exposed to cortisol, dobutamine (β_1-adrenergic receptor agonist) and terbutaline (β_2-adrenergic receptor agonist). A concentration of 0.01-1 µM cortisol induced a significant reduction in fluorescence anisotropy (Figure 3.2.2.1-1 and Table 3.2.2.1-1). For DPH fluorescence anisotropy values of 0.927 ± 0.021* for 0.01 µM cortisol, 0.928 ± 0.013*** for 0.1 µM cortisol and 0.889 ± 0.022*** for 1 µM cortisol were determined. For TMA-DPH a clear dose-dependent reduction to non-significant 0.997 ± 0.020, followed by significant 0.910 ± 0.015*** and 0.905 ± 0.014*** was observed for cortisol concentrations of 0.01, 0.1, and 1 µM, respectively.

For β-adrenergic agonists we could not observe changes in membrane fluidity using DPH and TMA-DPH after chronic exposure to 0.1 µM and 1 µM of terbutaline and dobutamine, respectively (Figure 3.2.2.1-2 and Table 3.2.2.1-2).

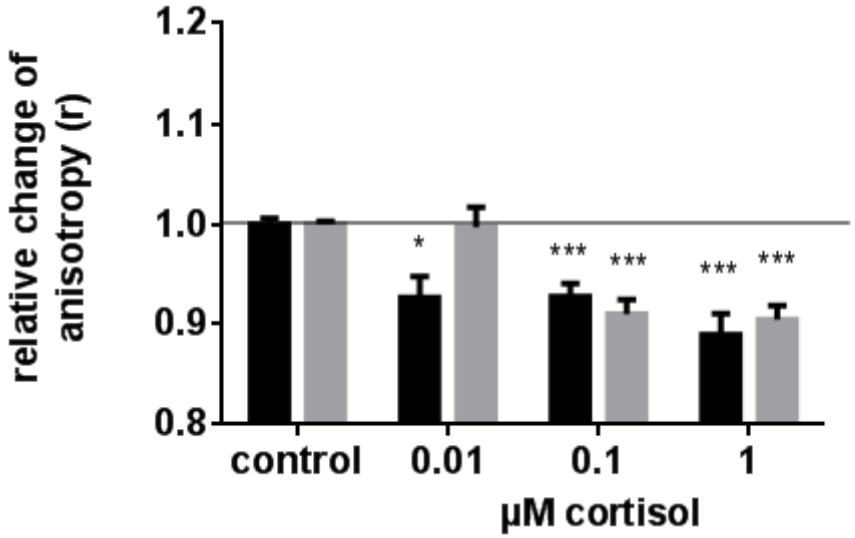

Figure 3.2.2.1-1: Relative changes in DPH (■) and TMA-DPH (■) fluorescence anisotropy of adherent C6 cells chronically exposed (6-8 days) to cortisol. Results are presented as mean ± SEM. Marked values ** p ≤ 0.01 and *** p ≤ 0.001 are significantly different from their corresponding controls, determined by the unpaired t-test. For corresponding values see Table 3.2.2.1-1.

Table 3.2.2.1-1: Corresponding values to Figure 3.2.2.1-1. Relative changes in DPH and TMA-DPH fluorescence anisotropy of adherent C6 cells chronically exposed (6-8 days) to cortisol.
Marked values ** p ≤ 0.01 and *** p ≤ 0.001 are significantly different from their corresponding controls, determined by the unpaired t-test.

	cortisol	mean ± SEM	n-value of samples	n-value of independent experiments
DPH	control	1.000 ± 0.006	25	15
	0.01 µM	0.927 ± 0.021*	7	5
	0.1 µM	0.928 ± 0.013***	16	9
	1 µM	0.889 ± 0.022***	8	6
TMA-DPH	control	1.000 ± 0.004	27	14
	0.01 µM	0.997 ± 0.020	7	4
	0.1 µM	0.910 ± 0.015***	12	6
	1 µM	0.905 ± 0.014***	13	7

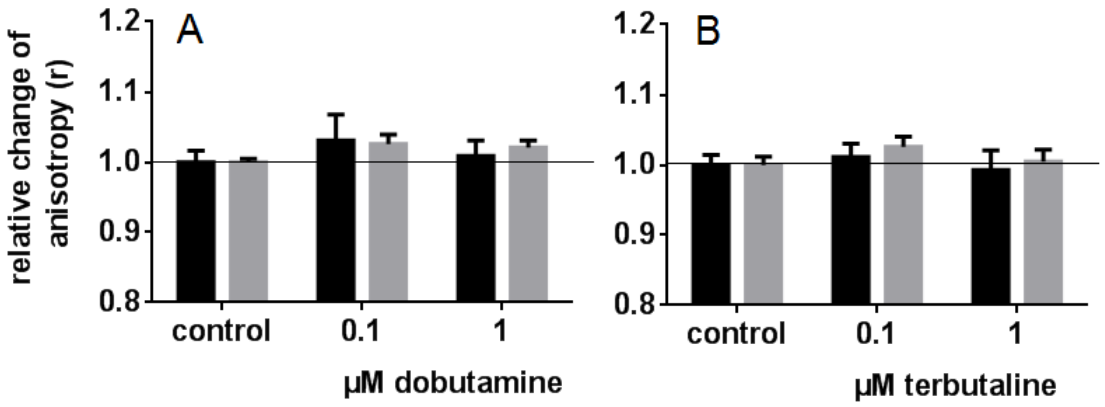

Figure 3.2.2.1-2: Relative changes in DPH (■) and TMA-DPH (■) fluorescence anisotropy of adherent C6 cells chronically exposed (6-8 days) to dobutamine or terbutaline. Results are presented as mean ± SEM. For corresponding values see Table 3.2.2.1-2.

Table 3.2.2.1-2: Corresponding values of Figure 3.2.2.1-2. Relative changes in DPH and TMA-DPH fluorescence anisotropy of adherent C6 cells chronically exposed (6-8 days) to 0.1 µM and 1 µM dobutamine or terbutaline.

	dobutamine	mean ± SEM	n-value of samples	n-value of independent experiments
DPH	control	1.000 ± 0.016	11	6
	0.1 µM	1.031 ± 0.037	5	4
	1 µM	1.009 ± 0.022	9	6
TMA-DPH	control	1.000 ± 0.005	12	6
	0.1 µM	1.026 ± 0.013	12	6
	1 µM	1.021 ± 0.010	11	6
	terbutaline	**mean ± SEM**	**n-value of samples**	**n-value of independent experiments**
DPH	control	1.000 ± 0.014	9	6
	0.1 µM	1.011 ± 0.019	9	6
	1 µM	0.993 ± 0.027	6	4
TMA-DPH	control	1.000 ± 0.012	8	4
	0.1 µM	1.026 ± 0.014	8	4
	1 µM	1.005 ± 0.017	7	4

3.2.2.2 Antidepressants

Testing the chronic influence of standard antidepressants citalopram (selective serotonin reuptake inhibitor (SSRI)) at a concentration of 1 µM did not affect DPH and TMA-DPH fluorescence anisotropy. On the other side chronic incubation with 1 µM desipramine (DMI, tricyclic antidepressant (TCA)) significantly increased DPH fluorescence anisotropy to 1.046 ± 0.008** compared to the corresponding control, while TMA-DPH fluorescence anisotropy was unchanged (Figure 3.2.2.2-1 and Table 3.2.2.2-1).

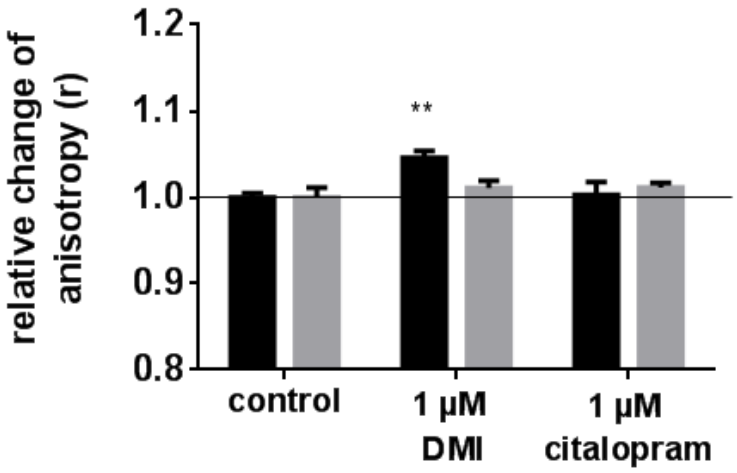

Figure 3.2.2.2-1: Relative changes in DPH (■) and TMA-DPH (■) fluorescence anisotropy of adherent C6 cells chronically exposed (6-8 days) to 1 µM DMI or 1 µM citalopram. Results are presented as mean ± SEM. For corresponding values see Table 3.2.2.2-1.

Table 3.2.2.2-1: Corresponding values to Figure 3.2.2.2-1. Relative changes in DPH and TMA-DPH fluorescence anisotropy of adherent C6 cells chronically exposed (6-8 days) to 1 µM DMI or citalopram.

	synthetic antidepressants	mean ± SEM	n-value of samples	n-value of independent experiments
DPH	control	1.000 ± 0.005	9	6
	1 µM DMI	1.046 ± 0.008**	6	4
	1 µM citalopram	1.003 ± 0.015	9	5
TMA-DPH	control	1.000 ± 0.017	10	5
	1 µM DMI	1.011 ± 0.009	10	5
	1 µM citalopram	1.011 ± 0.005	10	5

Chronic incubation with Ze117 significantly increased DPH and TMA-DPH fluorescence anisotropy values of in C6 cells after 6-8 days of pretreatment, compared to their control (Figure 3.2.2.2-2 and Table 3.2.2.2-2). Fluorescence anisotropy measurements using DPH achieved a dose-dependent increase to 1.080 ± 0.015**, 1.092 ± 0.013***, and 1.099 ± 0.010*** after incubation using concentrations of 0.01, 0.025, and 0.05 mg/ml Ze117, respectively. Identical incubation conditions revealed for TMA-DPH relative fluorescence anisotropy values of 1.041 ± 0.014*, 1.057 ± 0.013***, and 1.036 ±0.008**, respectively.

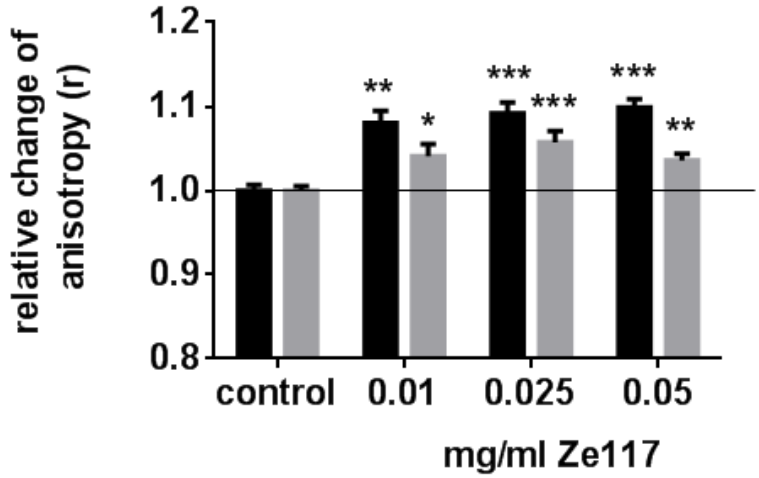

Figure 3.2.2.2-2: Relative change in DPH (■) and TMA-DPH (■) fluorescence anisotropy of adherent C6 cells chronically exposed (6-8 days) to the Hypericum perforatum dried extract Ze117. Results are presented as mean ± SEM. Marked values * p ≤ 0.05, ** p ≤ 0.01 and *** p ≤ 0.001 are significantly different from their corresponding controls, determined by the unpaired t-test. For corresponding values see Table 3.2.2.2-2.

Table 3.2.2.2-2: Corresponding values to Figure 3.2.2.2-2. Relative changes in DPH and TMA-DPH fluorescence anisotropy of adherent C6 cells chronically exposed (6-8 days) to Ze117. Marked values * p ≤ 0.05, ** p ≤ 0.01 and *** p ≤ 0.001 are significantly different from their corresponding controls, determined by the unpaired t-test.

	Ze117	mean ± SEM	n-value of samples	n-value of independent experiments
DPH	control	1.000 ± 0.006	25	15
	0.01 mg/ml	1.080 ± 0.015**	10	6
	0.025 mg/ml	1.092 ± 0.013***	13	8
	0.05 mg/ml	1.099 ± 0.010***	16	11
TMA-DPH	control	1.000 ± 0.005	28	14
	0.01 mg/ml	1.041 ± 0.014*	10	5
	0.025 mg/ml	1.057 ± 0.013***	15	9
	0.05 mg/ml	1.036 ± 0.008**	16	9

3.2.2.3 Bioactive ingredients of Ze117

For *Hypericum perforatum* a variety of bioactive ingredients have been described to contribute to the antidepressant effect, including hypericin, hyperforin and several flavonoids (*Linde, 2009*). Following chronic incubation (6-8 days) of C6 cells to such single substances an anisotropy increasing effect could be assigned at least to hypericin, hyperforin, quercetin, amentoflavone and biapigenin. With the exception to rutin, actually all tested substances induced an increase of the DPH and TMA-DPH fluorescence anisotropy compared to the control.

Chronic incubation (6-8 days) with hypericin at a concentration range of 0.01 µM and 0.1 µM mediated significantly increased DPH fluorescence anisotropy values dose-dependently to 1.039 ± 0.013*, and 1.079 ± 0.013***, while TMA-DPH fluorescence anisotropy reached values of 1.049 ± 0.016**, and 1.039 ± 0.012**, respectively. A concentration of 0.001 µM showed no effect (Figure 3.2.2.3-1A and Table 3.2.2.3-1).

Chronic incubation (6-8 days) with hyperforin gained a dose-dependent increase in DPH fluorescence anisotropy to 1.084 ± 0.033*, 1.053 ± 0.019*, and 1.108 ± 0.022*** by concentrations of 0.01 µM, 0.1 µM, and 1 µM. Parallel TMA-DPH fluorescence anisotropy measurements showed only at the highest concentration of 1 µM hyperforin a significantly increased value to 1.059 ± 0.013*** (Figure 3.2.2.3-1B and Table 3.2.2.3-1).

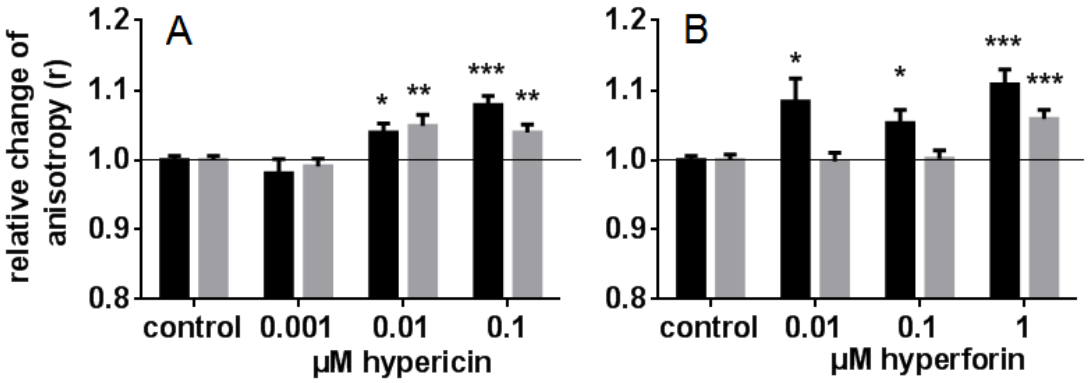

Figure 3.2.2.3-1: Relative change in DPH (■) and TMA-DPH (■) fluorescence anisotropy in adherent C6 cells after chronic incubation (6-8 days) with hypericin and hyperforin. Results are presented as mean ± SEM. Marked values * p ≤ 0.05, ** p ≤ 0.01 and *** p ≤ 0.001 are significantly different from their corresponding controls, determined by the unpaired t-test. For corresponding values see Table 3.2.2.3-1.

Table 3.2.2.3-1: Corresponding values to Figure 3.2.2.3-1. Relative changes in DPH and TMA-DPH fluorescence anisotropy of adherent C6 cells chronically exposed (6-8 days) to hypericin and hyperforin. Marked values * p ≤ 0.05, ** p ≤ 0.01 and *** p ≤ 0.001 are significantly different from their corresponding controls, determined by the unpaired t-test.

	hypericin	mean ± SEM	n-value of samples	n-value of independent experiments
DPH	control	1.000 ± 0.006	20	12
	0.001 µM	0.981 ± 0.020	6	4
	0.01 µM	1.039 ± 0.013*	8	6
	0.1 µM	1.079 ± 0.013***	14	11
TMA-DPH	control	1.000 ± 0.006	17	9
	0.001 µM	0.991 ± 0.011	10	5
	0.01 µM	1.049 ± 0.016**	10	6
	0.1 µM	1.039 ± 0.012**	13	7
	hyperforin	**mean ± SEM**	**n-value of samples**	**n-value of independent experiments**
DPH	control	1.000 ± 0.006	13	7
	0.01 µM	1.084 ± 0.033*	4	3
	0.1 µM	1.053 ± 0.019*	10	5
	1 µM	1.108 ± 0.022***	7	4
TMA-DPH	control	1.000 ± 0.008	19	10
	0.01 µM	0.998 ± 0.012	9	5
	0.1 µM	1.002 ± 0.012	16	9
	1 µM	1.059 ± 0.013***	16	9

Chronic exposure (6-8 days) of C6 cells to the flavonoid quercetin in concentrations of 0.5 µM, 1 µM, and 1.5 µM induced an dose-dependent increase of the relative DPH fluorescence anisotropy to 1.016 ± 0.028 and statistical significant 1.067 ± 0.019* and 1.112 ± 0.012**, respectively. The same concentrations of 0.5 - 1.5 µM quercetin changed the TMA-DPH fluorescence anisotropy to 1.031 ± 0.016, 1.032 ± 0.008***, and statistically significant 1.028 ± 0.012*, compared to their corresponding controls (Figure 3.2.2.3-2B and Table 3.2.2.3-2). Rutin, which was tested at a concentration of 1 µM, showed no changes (Figure 3.2.2.3-2A and Table 3.2.2.3-2).

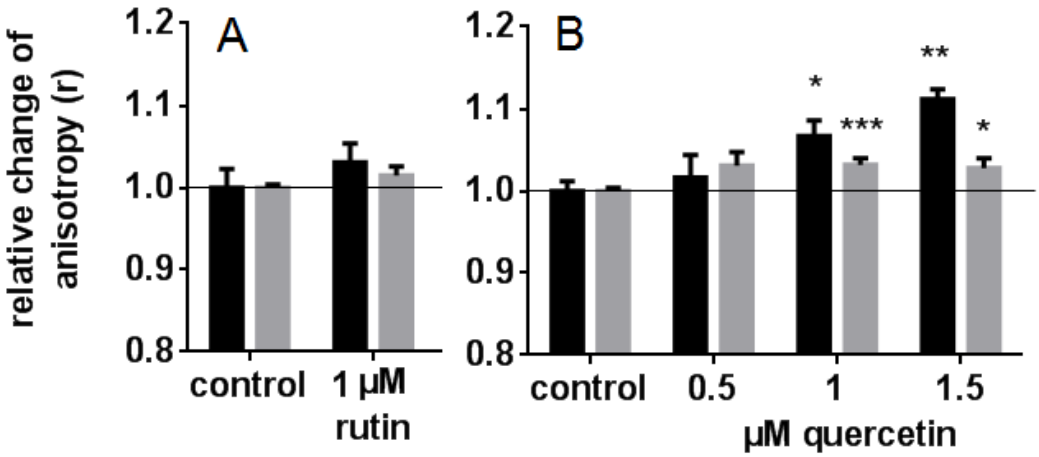

Figure 3.2.2.3-2: Relative changes in DPH (▬) and TMA-DPH (▬) fluorescence anisotropy values of adherent C6 cells chronically exposed (6-8 days) to rutin or quercetin. Results were pooled and are presented as mean ± SEM. Marked values * p ≤ 0.05, ** p ≤ 0.01 and *** p ≤ 0.001 are significantly different from their corresponding controls, determined by the unpaired t-test. For corresponding values see Table 3.2.2.3-2.

Table 3.2.2.3-2: Corresponding values to Figure 3.2.2.3-2. Relative changes in DPH and TMA-DPH fluorescence anisotropy of adherent C6 cells chronically exposed (6-8 days) to rutin or quercetin. Marked values * p ≤ 0.05, ** p ≤ 0.01 and *** p ≤ 0.001 are significantly different from their corresponding controls, determined by the unpaired t-test.

	rutin	mean ± SEM	n-value of samples	n-value of independent experiments
DPH	control	1.000 ± 0.020	10	6
	1 µM	1.031 ± 0.023	9	6
TMA-DPH	control	1.000 ± 0.004	20	11
	1 µM	1.015 ± 0.011	19	11
	quercetin	**mean ± SEM**	**n-value of samples**	**n-value of independent experiments**
DPH	control	1.000 ± 0.012	26	15
	0.5 µM	1.016 ± 0.028	5	3
	1 µM	1.067 ± 0.019*	11	7
	1.5 µM	1.112 ± 0.012**	9	7
TMA-DPH	control	1.000 ± 0.004	40	20
	0.5 µM	1.031 ± 0.016	10	5
	1 µM	1.032 ± 0.008***	21	12
	1.5 µM	1.028 ± 0.012*	16	9

The biflavonoid amentoflavone, which was also examined at a concentration range of 0.5 - 1.5 µM exposed a dose-dependent increase in DPH fluorescence anisotropy, which reached statistical significance at the highest concentration of 1.5 µM with an increase to 1.082 ± 0.033*. Statistical significance was also seen in TMA-DPH fluorescence anisotropy, which reached a value of 1.041 ± 0.013* after chronic incubation to 1.5 µM amentoflavone (Figure 3.2.2.3-3A and Table 3.2.2.3-3).

Chronic incubation (6-8 days) with the biflavonoid biapigenin showed statistic significant alterations of DPH fluorescence anisotropy to 1.087 ± 0.018** by 1 µM and 1.101 ± 0.016** by 1.5 µM. For TMA-DPH no effect was observed compared to the control (Figure 3.2.2.3-3B and Table 3.2.2.3-3).

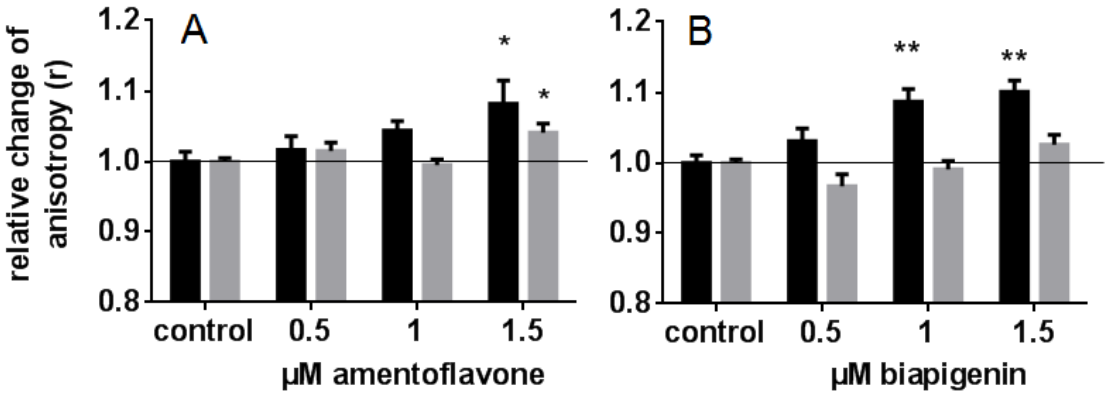

Figure 3.2.2.3-3: Relative changes in DPH (■) and TMA-DPH (■) fluorescence anisotropy values of adherent C6 cells chronically exposed (6-8 days) to amentoflavone or biapigenin. Results are presented as mean ± SEM. Marked values ** $p \leq 0.01$ and *** $p \leq 0.001$ are significantly different from their corresponding controls, determined by the unpaired t-test. For corresponding values see Table 3.2.2.3-3.

Table 3.2.2.3-3: Corresponding values to Figure 3.2.2.3-3. Relative changes in DPH and TMA-DPH fluorescence anisotropy of adherent C6 cells chronically exposed (6-8 days) to amentoflavone or biapigenin. Marked values ** p ≤ 0.01 and *** p ≤ 0.001 are significantly different from their corresponding controls, determined by the unpaired t-test.

	amentoflavone	mean ± SEM	n-value of samples	n-value of independent experiments
DPH	control	1.000 ± 0.014	30	17
	0.5 µM	1.016 ± 0.020	6	4
	1 µM	1.044 ± 0.013	8	5
	1.5 µM	1.082 ± 0.033*	11	7
TMA-DPH	control	1.000 ± 0.005	40	21
	0.5 µM	1.015 ± 0.012	11	6
	1 µM	0.995 ± 0.008	19	11
	1.5 µM	1.041 ± 0.013*	12	7
	biapigenin	**mean ± SEM**	**n-value of samples**	**n-value of independent experiments**
DPH	control	1.000 ± 0.011	25	16
	0.5 µM	1.031 ± 0.017	7	4
	1 µM	1.087 ± 0.018**	12	8
	1.5 µM	1.101 ± 0.016**	8	5
TMA-DPH	control	1.000 ± 0.005	29	15
	0.5 µM	0.967 ± 0.017	9	5
	1 µM	0.991 ± 0.012	16	9
	1.5 µM	1.026 ± 0.014	8	4

3.2.2.4 Acute incubation of C6 cells

To proper distinguish between a chronic and a possible direct membrane interacting effect associated with changes in membrane fluidity an additional acute exposure approach was performed. Adherent C6 cells were treated for 1 h with several substances under investigation. The following washing, background determination, DPH or TMA-DPH labeling and measurement procedure were identical for both, the acute and the chronic approach. With the exception of cortisol, all substances under investigation showed no direct membrane-interacting mediated effect on DPH and TMA-DPH fluorescence anisotropy (Figure 3.2.2.4 and Table 3.2.2.4). Acute incubation with 1 µM cortisol induced a small but significant increased TMA-DPH fluorescence anisotropy value to 1.033 ± 0.011**.

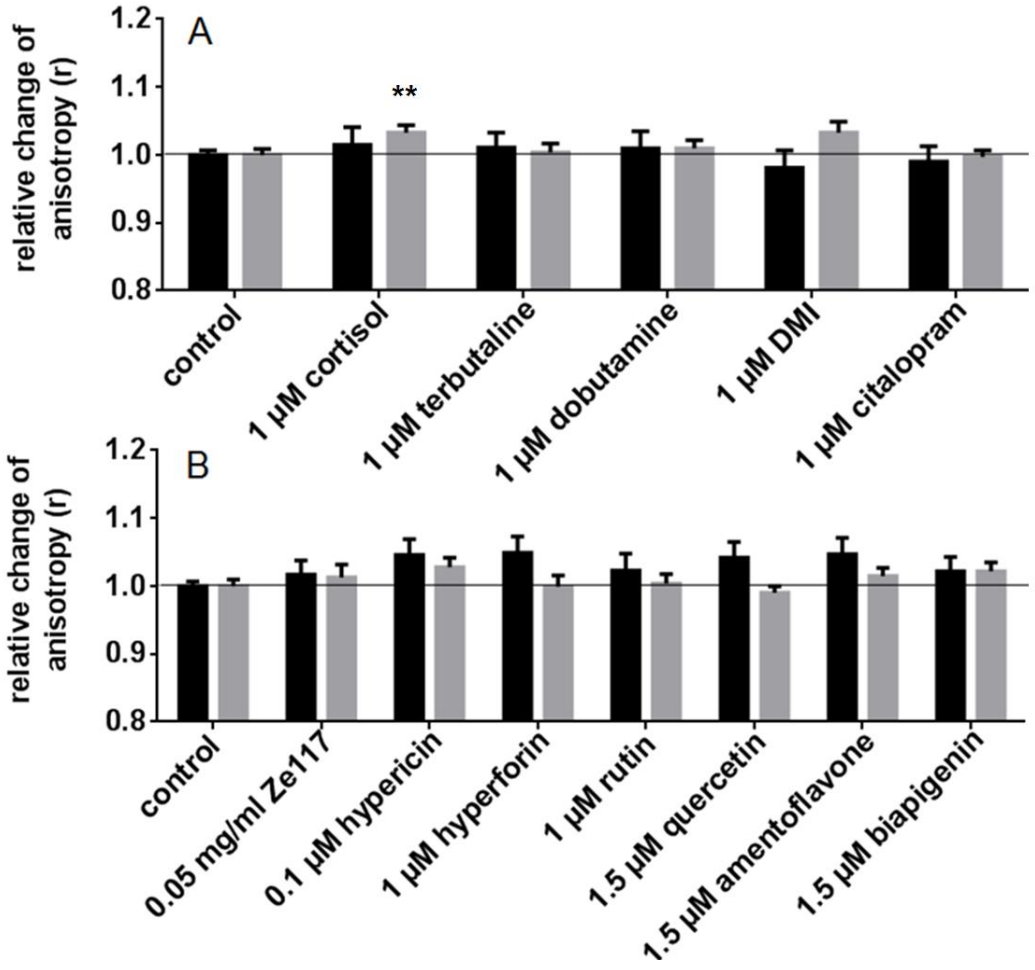

Figure 3.2.2.4: Relative changes in DPH (■) and TMA-DPH (■) fluorescence anisotropy values of adherent C6 cells after acute exposer (1 h) to several test substances under investigation. Results are presented as mean ± SEM. Marked values ** $p \leq 0.01$ are significantly different from their corresponding controls, determined by the unpaired t-test. For corresponding values see Table 3.2.2.4

Table 3.2.2.4: Correspondng values to Figure 3.2.2.4. Relative changes in DPH and TMA-DPH fluorescence anisotropy of adherent C6 cells acutely exposed for 1h to several substances under investigation.

	control substances	mean ± SEM	n-value of samples	n-value of independent experiments
DPH	control	1.000 ± 0.007	19	10
	1 µM cortisol	1.015 ± 0.026	14	8
	1 µM terbutaline	1.011 ± 0.022	11	7
	1 µM dobutamine	1.010 ± 0.025	11	7
	1 µM DMI	0.981 ± 0.026	15	9
	1 µM citalopram	0.990 ± 0.023	11	6
TMA-DPH	control	1.000 ± 0.009	22	10
	1 µM cortisol	1.033 ± 0.011**	14	7
	1 µM terbutaline	1.004 ± 0.013	9	5
	1 µM dobutamine	1.010 ± 0.012	10	5
	1 µM DMI	1.033 ± 0.016	14	7
	1 µM citalopram	0.997 ± 0.010	13	7
	Ze117 and ingredients	**mean ± SEM**	**n-value of samples**	**n-value of independent experiments**
DPH	control	1.000 ± 0.007	19	10
	0.05 mg/ml Ze117	1.017 ± 0.021	11	6
	0.1 µM hypericin	1.046 ± 0.023	11	7
	1 µM hyperforin	1.049 ± 0.024	11	6
	1µM rutin	1.023 ± 0.025	11	8
	1.5 µM quercetin	1.042 ± 0.023	12	7
	1.5µM amentoflavone	1.047 ± 0.024	14	8
	1.5 µM biapigenin	1.022 ± 0.021	11	6
TMA-DPH	control	1.000 ± 0.010	20	9
	0.05 mg/ml Ze117	1.013 ± 0.019	16	8
	0.1 µM hypericin	1.028 ± 0.014	14	7
	1 µM hyperforin	0.999 ± 0.017	15	8
	1 µM rutin	1.004 ± 0.014	11	6
	1.5 µM quercetin	0.990 ± 0.010	16	8
	1.5 µM amentoflavone	1.015 ± 0.012	10	6
	1.5 µM biapigenin	1.022 ± 0.013	11	6

3.3 Assessment of changes within the PC/PE ratio of C6 cells by TLC

To examine possible changes within the phospholipid composition, associated to membrane fluidity changes, we investigated the phosphatidylcholine to phosphatidylethanolamine (PC/PE) ratio of C6 cells using thin layer chromatography (TLC). In comparison to control we found a significant increase in the PC/PE ratio to 1.343 ± 0.078*** following chronic incubation (6 days) with 10 mM choline and a significant reduction in the PC/PE ratio to 0.819 ± 0.075** after chronic treatment with 1 µM cortisol. Ze117 also revealed a reducing effect on the PC/PE ratio. This effect was dose-dependent for the analyzed concentrations of 0.01 - 0.05 mg/ml and reached statistical significance at the highest concentration of 0.05 mg/ml Ze117 with 0.866 ± 0.055**. In contrast, chronic treatment with 1 µM DMI and 1 µM citalopram did not affect the PC/PE ratio (Figure 3.3 and Table 3.3).

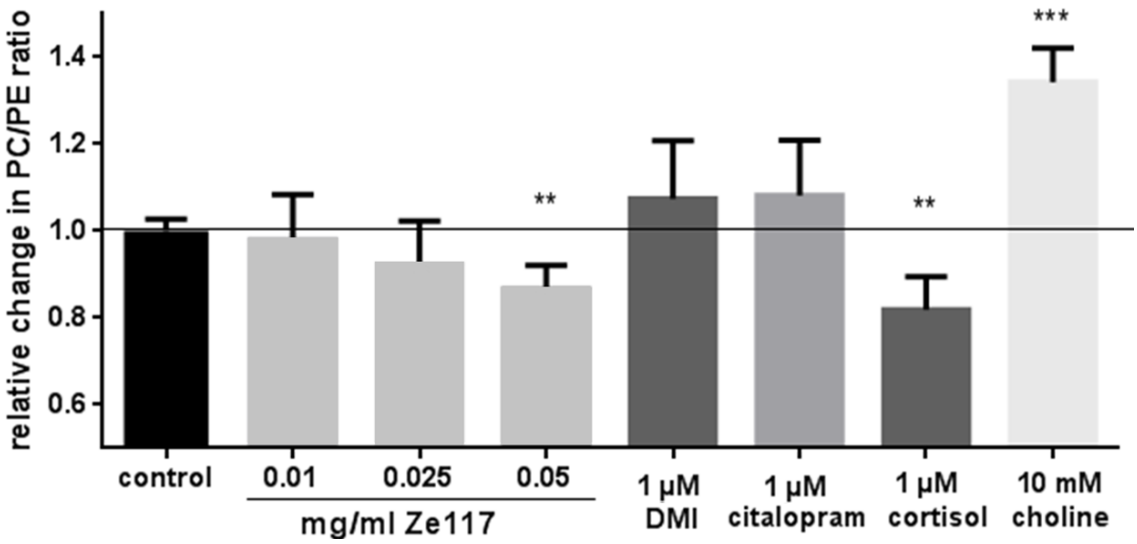

Figure 3.3: Relative change in the PC/PE ratio within whole cell lipid extracts derived from C6 cells chronically incubated (6 days) with 1 µM cortisol, 1 µM DMI, 1 µM citalopram or 0.01-0.05 mg/ml Ze117, determined by densitometric TLC. Results are presented as mean ± SEM. Marked values ** $p \leq 0.01$ and *** $p \leq 0.001$ are significantly different from their corresponding controls, determined by the unpaired t-test. For corresponding values see Table 3.3.

Table 3.3: Corresponding values of Figure 3.3. Relative change in the PC/PE ratio within whole cell lipid extracts derived from C6 cells chronically treated (6 days) with 1 µM cortisol, 1 µM DMI, 1 µM citalopram, or 0.01 - 0.05 mg/ml Ze117 analyzed by densitometric TLC. Marked values ** $p \leq 0.01$ are significantly different from their corresponding controls, determined by the unpaired t-test.

	mean ± SEM	n-value of samples
Control	1.000 ± 0.027	13
0.01 mg/ml Ze117	0.980 ± 0.104	5
0.025 mg/ml Ze117	0.923 ± 0.099	4
0.05 mg/ml Ze117	0.866 ± 0.055**	5
1 µM DMI	1.074 ± 0.133	4
1 µM citalopram	1.082 ± 0.127	4
1 µM cortisol	0.819 ± 0.075**	4
10 mM choline	1.343 ± 0.078***	4

3.4 PC pulse-chase and PC identification

Observing a generally reduced PC/PE ratio after chronic exposure to cortisol and Ze117 we focused closer to the question whether a suggested reduction in PC may result from a general reduction of the whole PC pool or a selective reduction affecting only specific PC species. This question was experimentally approached by exposure of C6 cells to 50 µM choline-D9 for 24 h, which becomes incorporated into PC via the de-novo biosynthesis pathway and subsequently is detectable by mass spectrometric analysis. As presented in Figure 3.4-1 mass spectrometric analysis allowed the detection of the most prominent PC species ($[M+H]^+$) with m/z = 732, 754, 758, 760, 782, 786, and 808 by the appearance of their deuterated derivatives with m/z = 741, 763, 767, 769, 791, 795, and 817 within whole cell lipid extracts.

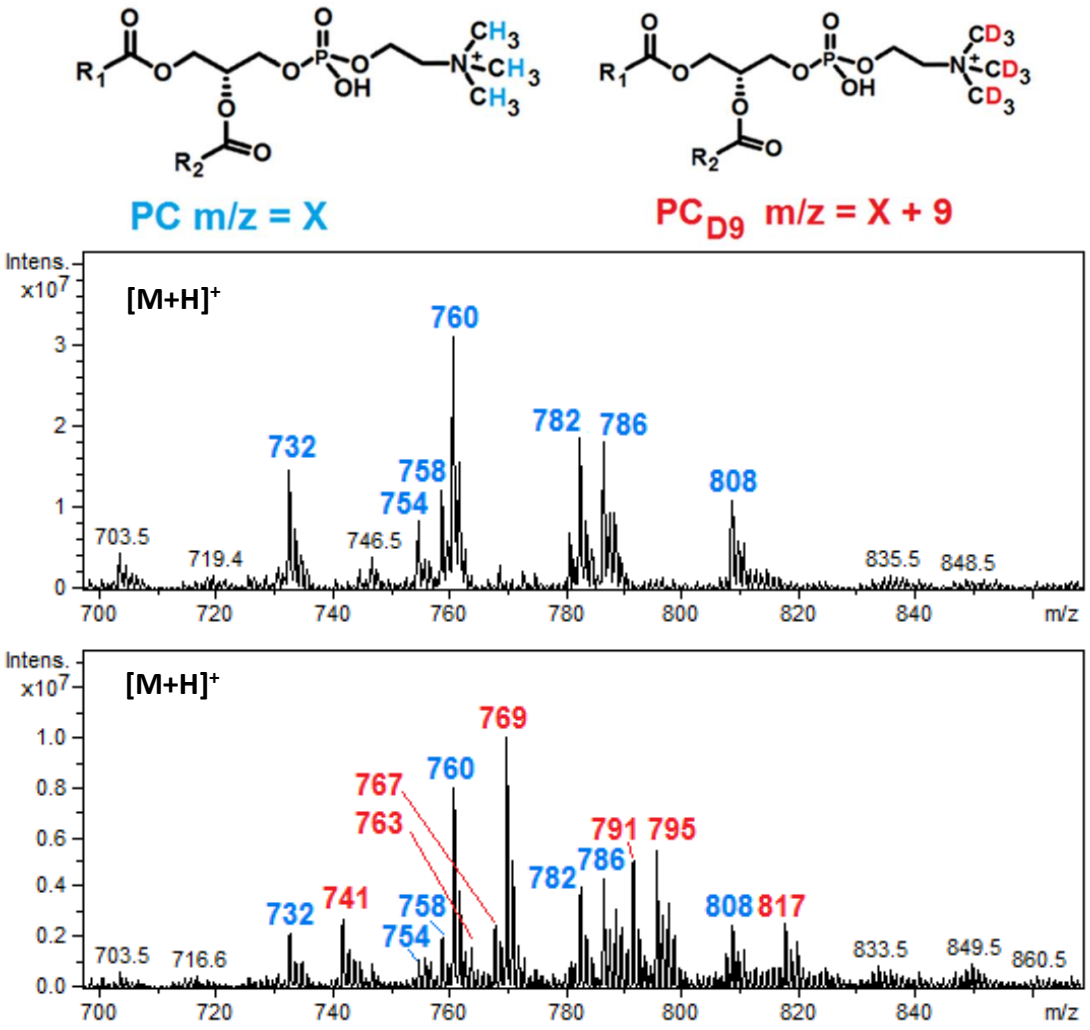

Figure 3.4-1: Positive mode mass spectra of whole cell lipid extracts derived from C6 control cells with and without 24 h exposure to 50 µM choline-D9. The incorporation of choline-D9 into PC via the de-novo biosynthesis pathway results in the appearance of deuterated PC derivatives (**red**) of corresponding natural occurring PC species (**blue**). These PC pairs expose a mass difference of 9 resulting from the 3 deuterated methyl groups of choline-D9.

The identities of these pairs as PC species were confirmed by positive mode MS2 fragmentation (+MS2) (Table 3.4-1 and appendix, Figure 6.1). Neutral loss of the head group (phosphocholine with m/z = 183, phosphocholine-D9 with m/z = 192) results in the presence of a diacylglycerol (DAG)-like fragment which is identical for the natural and the deuterated PC species (Figure 3.4-2). Neutral loss of choline (with m/z = 59) or choline-D9 (with m/z = 68 m/z) from the parent ion was also examined.

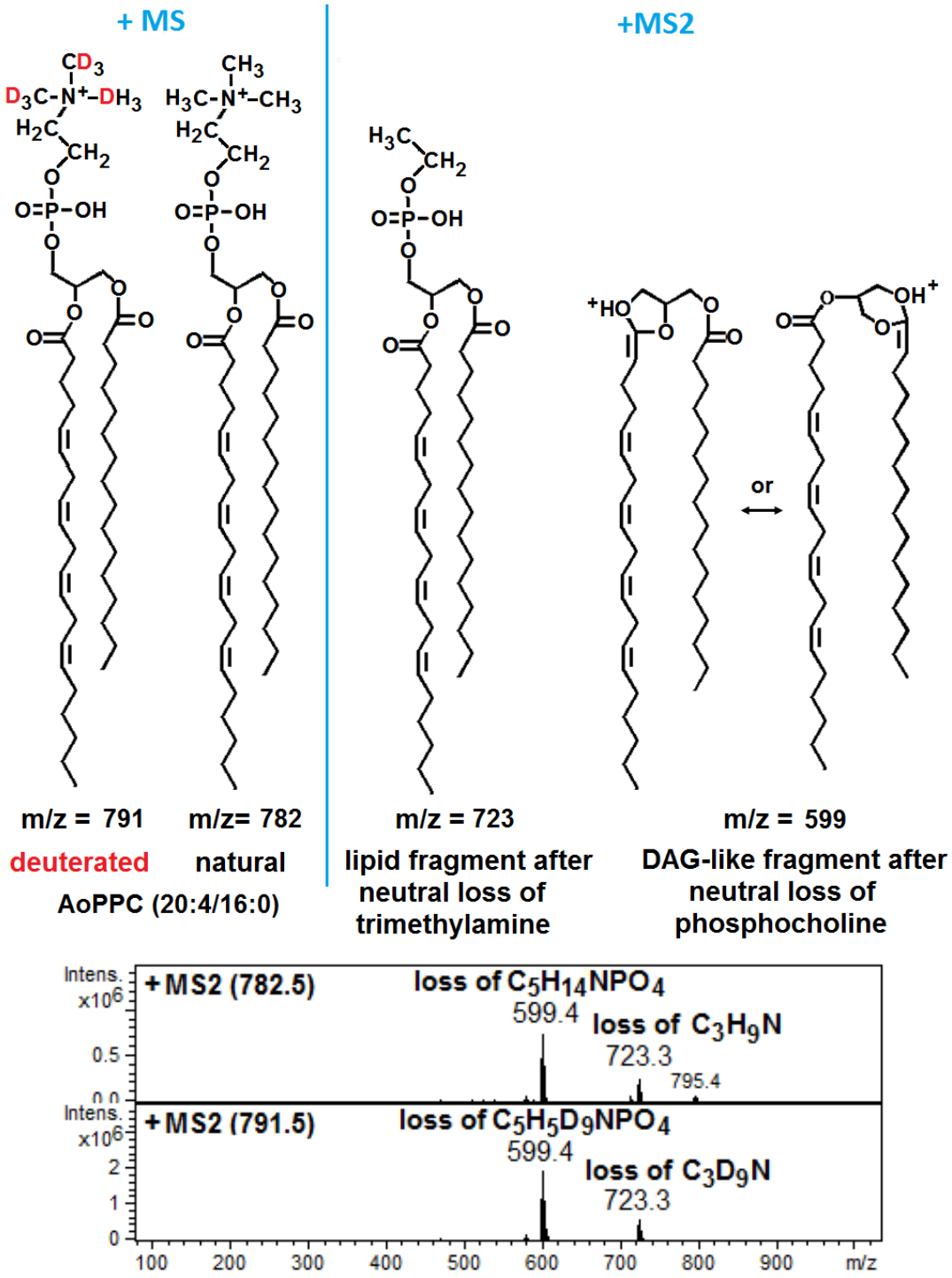

Figure 3.4-2: Positive mode fragmentation principle of PC pairs presented on the example of AoPPC (20:4/16:0). (Upper panel) Natural occurring PC species and their deuterated derivatives were identified as PC pair within +MS2 by forming an identical DAG-like fragment by neutral loss of the head group (phosphocholine with m/z = 183, phosphocholine-D9 with m/z = 192). The loss of choline (-59 m/z) or choline-D9 (-68 m/z) from the parent ion can also be examined. Adapted from *www.byrdwell.com/PhosphatidylCholine/PCfragments*
(Lower panel) corresponding +MS2 spectrum.

Tabele 3.4-1: Conformation of main species and their deuterated derivatives as actual PC species, performed by positive mode MS2 fragmentation. PC-pairs are identified within the +MS2 by forming an identical DAG-like fragment by neutral loss of the head group (phosphocholine with m/z = 183, phosphocholine-D9 with m/z = 192 m/z). The loss of choline (with m/z = 59) or choline-D9 (with m/z = 68) from the parent ion can also be examined.

+MS		+MS2	
[M+H]+		DAG-like fragment after neutral loss of head group	PC fragment after neutral loss of trimethylamine
732 741	→	549 549	673 673
754 763	→	571 571	695 695
758 767	→	575 575	699 699
760 769	→	577 577	701 n.d.
782 791	→	599 599	723 723
786 795	→	603 603	727 727
808 817	→	625 625	749 749

n.d. = not detected

Approaching changed synthesis kinetics of these main PC species after chronic treatment (6 days) with antidepressants and cortisol, C6 cells were co-exposed to 50 µM choline-D9 for the last 24 h of incubation. Chronic incubation (6 days) with 1 µM DMI, 1 µM citalopram or 1 µM cortisol showed no significant alteration in the choline-D9 incorporation rate within the examined main PC species, compared to control (Table 3.4-2). Following chronic incubation with 0.05 mg/ml Ze117 a significant reduction of the choline-D9 content was observed within specific PC species with m/z = 732, 758, 760, and 786. In detail, the choline-D9 bearing PC content was reduced for the PC species with m/z = 732 by 24% (from 50.8% to 38.5%***), m/z = 758 by 37% (from 47.5% to 30.1%***), m/z = 760 by 17% (from 52.4 to 43.7%***), and m/z = 786 by 9% (from 53.5% to 48.7%**) (Table 3.4-2).

Table 3.4-2: Deuterated content in percent within main PC species after 24 h co- exposure to 50 µM choline-D9 of C6 cells chronically incubated (6 days) with Ze117, antidepressants or cortisol. Marked values ** p ≤ 0.01 and *** p ≤ 0.001 are significantly different from their corresponding controls determined by the unpaired t-test. .

$[M+H]^+$		732_{D9}	754_{D9}	758_{D9}	760_{D9}	782_{D9}	786_{D9}	808_{D9}
Control	mean	50.8	58.3	47.5	52.4	55.7	53.5	53.2
	SEM	± 0.75	± 0.66	± 1.02	± 0.53	± 0.60	± 0.49	± 0.57
	N	16	16	13	16	16	16	16
Ze117 0.05 mg/ml	mean	38.5***	57.1	30.1***	43.7***	54.3	48.7**	51.1
	SEM	± 1.45	± 2.72	± 1.35	± 1.08	± 1.94	± 1.28	± 1.82
	N	7	6	7	7	7	7	7
DMI 1 µM	mean	50.6	57.3	47.1	50.9	53.3	51.3	52.5
	SEM	± 0.92	± 0.81	± 1.35	± 1.30	± 1.12	± 0.90	± 1.46
	N	6	6	5	6	6	6	6
Citalopram 1 µM	mean	51.1	58.2	47.0	51.9	54.6	51.9	53.0
	SEM	± 1.90	± 0.55	± 2.55	± 1.38	± 0.44	± 1.41	± 1.04
	N	5	5	5	5	5	5	5
Cortisol 1 µM	mean	49.4	58.0	44.9	49.8	53.9	49.9	52.8
	SEM	± 1.67	± 0.71	± 2.15	± 1.15	± 0.34	± 1.08	± 0.54
	N	7	7	6	7	7	7	7

Subsequent these PC-species become characterized by their fatty acid composition by negative mode fragmentation (Figure 3.4-4) which allowed the identification of these PC species affected by Ze117 as PPoPC (16:0/16:1), MOPC (14:0/18:1), PoOPC (16:1/18:1), POPC (16:0/18:1), and Di-OPC (18:1/18:1) (Table 3.4-4 and appendix, Figure 6.2). The remaining PC species, not affected by Ze117, have been identified as polyunsaturated fatty acid (PUFA) bearing PC species with m/z = 782 represents PAoPC (16:0/20:4) and PohLPC (16:1/20:3) and m/z = 808 could be identified as OAoPC (18:1/20:4). These PUFA bearing PC species were observed with a much lower abundancy within the negative mode, compared to positive mode MS spectra (compare Figure 3.4-1 and Figure 3.4-3). As a consequence of this phenomenon the PC species with m/z = 754 $[M+H]^+$, which had already the lowest intensity within the positive mode, became undetectable within negative mode observations. However, online data base analysis strongly suggest the PC species PoLnPC (16:1/18:3) to be presented by m/z = 754 $[M+H]^+$ as the PC species bearing the fatty acid combination 16:0/18:4 is rare.

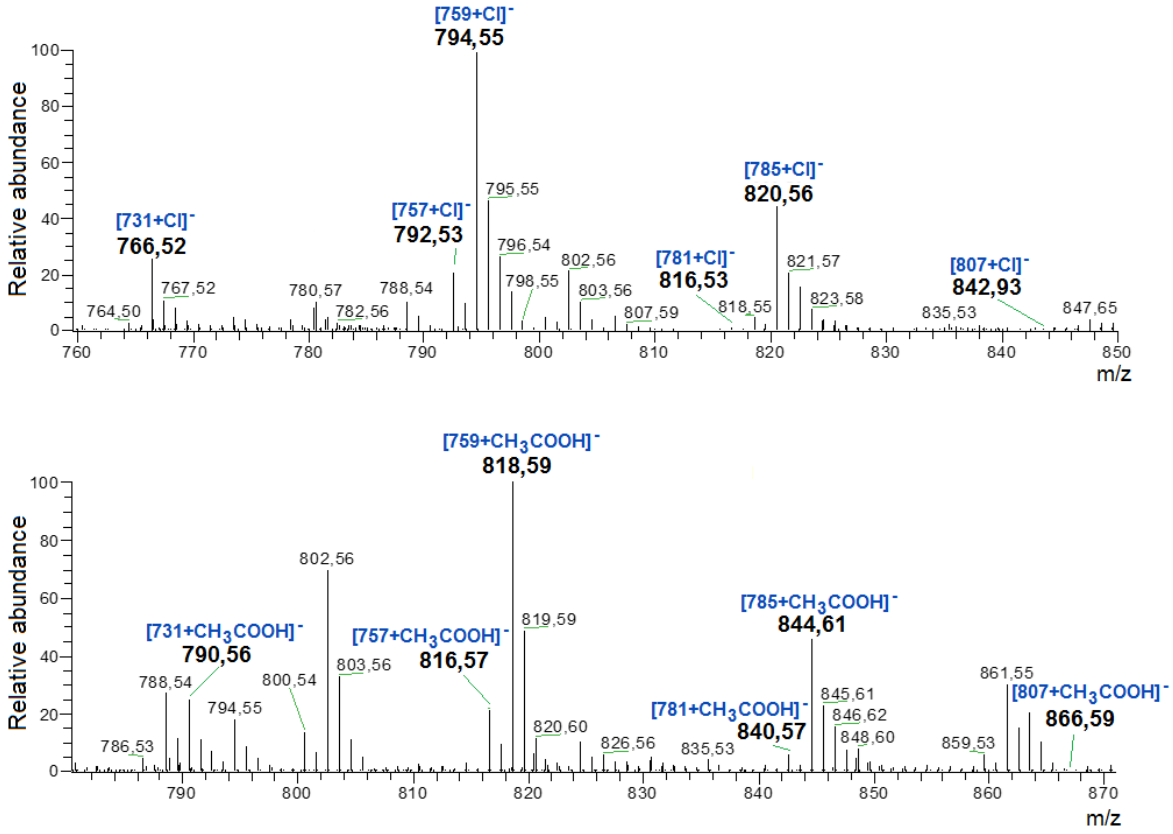

Figure 3.4-3: Negative mode mass spectrum of whole cell lipid extracts derived from C6 cells. Main PC species previously investigated at positive mode as $[M+H]^+$ cations are detected within the negative mode as anionic chloride $[M+Cl]^-$ **(upper panel)** or acetate $[M+CH_3COO]^-$ adduct **(lower panel)**. The PC species with m/z = 754 $[M+H]^+$ calculated to expose a m/z of 812 $[M+CH_3COO]^-$ was not detected within negative mode observations. The corresponding $[M+Cl]^-$ adduct calculated to expose a m/z of 788, if present overlies with phosphatidylserine (18:0/18:1) at 788.54 m/z present in both negative mode spectra.

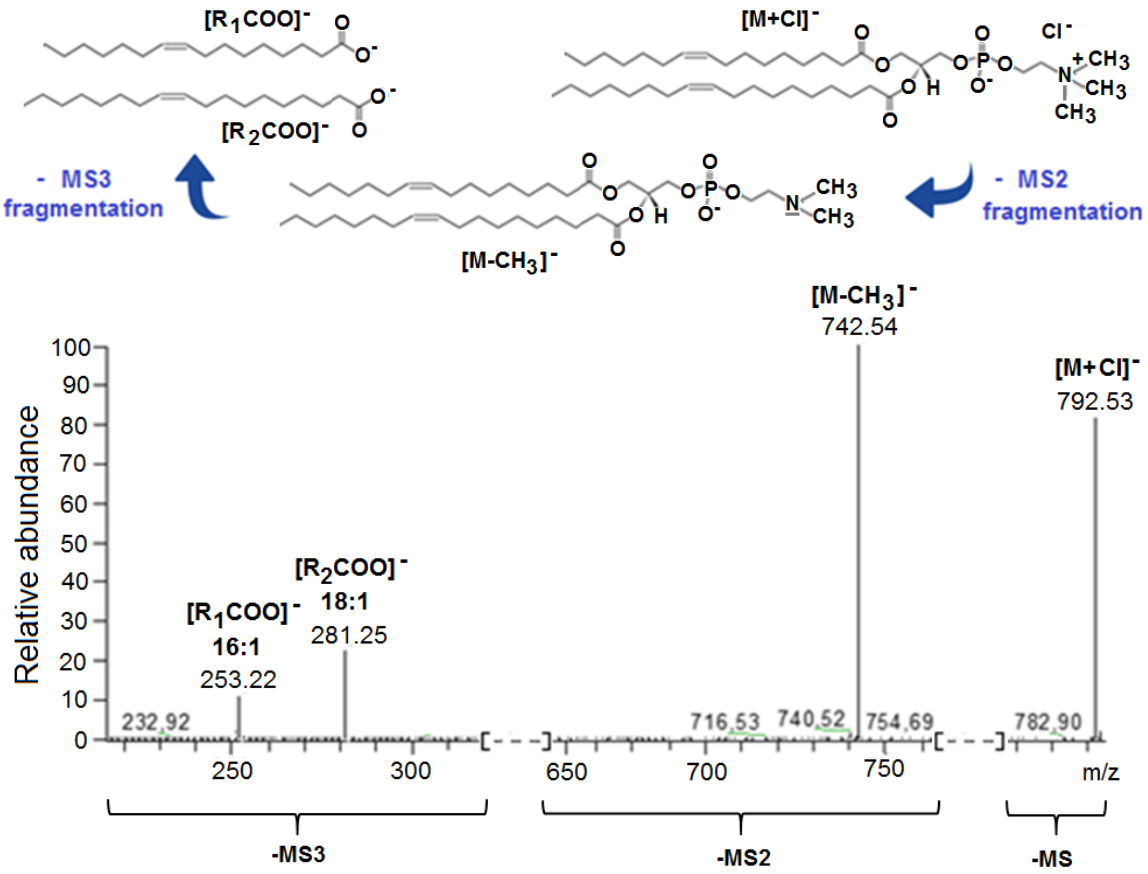

Figure 3.4-4: Negative mode fragmentation of anionic PC adducts for fatty acid identification. Fragmentation presented by the example of the PoOPC (16:1/18:1) chloride adduct. The PC adduct becomes fragmented resulting in a $[M\text{-}CH_3]^-$ fragment, which is further fragmented allowing fatty acid identification. The sn-2 fatty acid fragment $[R_2COO]^-$ is distinguished from the sn-1 fatty acid fragment $[R_1COO]^-$ due to it appears with a higher abundancy within the MS3 spectrum.

Table 3.4-3: PC species identification. Parental masses of examined main PC species within the positive mode allowed assumption of possible fatty acid combinations.
Actual fatty acid composition was examined by negative mode MS3 (- MS3) fragmentation of $[M+Cl]^-$ or $[M+CH_3COO]^-$ according to Figure 3.4-4.

+MS		- MS3			PC species
Parental mass	**Possible PC species***	**Fatty acid fragment**			**Identified**
732	PPoPC (16:0 /16:1) MOPC (14:0/18:1)	→	227 (14:0) 253 (16:1) 255 (16:0) 281 (18:1)	→	PPoPC (16:0/16:1) MOPC (14:0/18:1)
754	PoLnPC (16:1/18:3)	→	n.d.	→	
758	PLPC (16:0 /18:2) PoOPC (16:1/18:1)	→	281 (18:1) 253 (16:1)	→	PoOPC (16:1/18:1)
760	POPC (16:0/18:1) PoSPC (16:1/18:0)	→	281 (18:1) 255 (16:0)	→	POPC (16:0/18:1)
782	PAoPC (16:0/20:4) PohLPC (16:1/20:3) Di-LPC (18:2/18:2)	→	255 (16:0) 253 (16:1) 305 (20:3) 303 (20:4)	→	PAoPC (16:0/20:4) PohLPC (16:1/20:3)
786	PoGPC (16:1/20:1) SLPC (18:0/18:2) Di-OPC (18:1/18:1)	→	281 (18:1)	→	Di-OPC(18:1/18:1)
808	OAoPC (18:1/20:4) LhLPC (18:2/20:3)	→	281 (18:1) 303 (20:4)	→	OAoPC (18:1/20:4)

M; myristic acid (14:0), P; palmic acid (16:0), Po; palmitoleic acid (16:1), S; stearic acid (18:0), O; oleic acid or elaidic acid (18:1), L; linoleic acid (18:2), Ln; linolenic acid (18:3), G; gadoleic acid or gondoic acid (20:1), hL; homo-g-linolenic (20:3), Ao; arachidonic acid (20:4).

* www.byrdwell.com/PhosphatidylCholine/FattyAcids

n.d. = *not detected*

4 Discussion

4.1 DPH and TMA-DPH fluorescence anisotropy measurements in adherent C6 cells

Within this study, changes of the plasma membrane fluidity of C6 cells were assessed by fluorescence anisotropy measurements. For this approach DPH (1,6-diphenyl-1,3,5-hexatriene) and its derivative TMA-DPH (1-(4-(trimethylamino)phenyl)-6-phenylhexa-1,3,5-triene) were applied as fluorescent probes which spontaneously partitioning into the membrane and gauge the movement of their surrounding microenvironment. The DPH molecule is one of the most favorable probes for polarization studies due its low solubility and quenched emission in water (*Lakowicz, 2006; Li et al., 2000; Loura & Ramalho 2011).* DPH is readily soluble in the hydrocarbon core, where the fluorescence originates from the hydrophobic milieu within deeper portions of the membrane bilayer (*Aricha et al., 2004; Lakowicz, 2006; Repakova et al., 2005*). The orientation of DPH within the membrane is favored parallel to the middle region of the hydrocarbon acyl chains of the phospholipids of the outer bilayer leaflet (Figure 4.1) (*Aricha et al., 2004; Repakova et al., 2005; Nelson et al., 2012; Fraňová et al., 2010*). This orientation of the rod like structured molecule makes DPH very sensitive to changes of the angular reorientation of the long axis of the neighboring lipophilic acyl chain environment *(Loura & Ramalho, 2011; Aricha et al., 2004*). The DPH derivative TMA-DPH was designed to anchor itself with its charged trimethylammonium group to the membrane/water interface. TMA-DPH is therefore proposed to allow the determination of rotational changes more close to the phospholipid head group region (*do Canto et al., 2016*; Fišar et al., 2005).

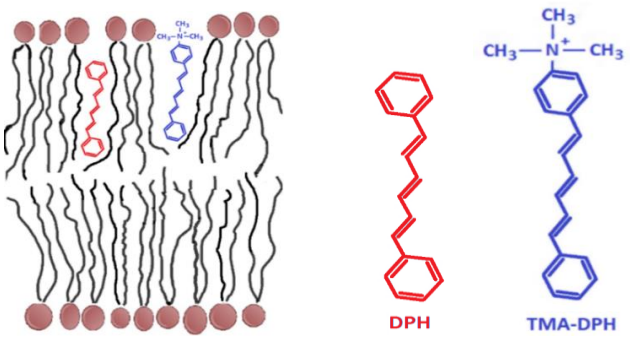

Figure 4.1: Chemical structure and schematic membrane incorporation of DPH and TMA-DPH.

Fluorescence anisotropy measurements were performed on adherent C6 cells applying an incident light angle of 30° relative to the cell monolayer. This angle directs reflected light away from the detector leading to minimized background signal (Bkg) and more reliable anisotropy measurements, compared to the usually used “magic angle” of 45° (*Sumbilla & Lakowicz, 1983; Lakowicz 2006*). In order to allow accurate interpretation of DPH and TMA-DPH fluorescence anisotropy changes, this experimental setup was finally evaluated by membrane fluidity manipulation.

In order to examine the actual sensitivity of TMA-DPH to membrane fluidity changes within the phospholipid head group region selective enrichment of the phosphatidylcholine (PC) content was performed by increasing choline availability, which as the starting substrate of the PC de-novo pathway becomes incorporated as the choline head group (*Jamil & Vance, 1990; Fagone & Jackowski, 2013*). Following chronic incubation of C6 cells with choline a significant increase of the PC/PE ratio by 33 % within whole cell lipid extracts correlated to a small but significantly decreased TMA-DPH fluorescence anisotropy value. These observation correlates to what is described in literature for the relationship between membrane fluidity and PC/PE ratio (*Fajardo et al., 2011*).

PC represents a main bilayer-forming phospholipid class, making up to 50 % of the phospholipid content (*van Meer, 2005; Mitchel et al., 2007*). The spatial cylindrical shaped choline head group and its hydration status negates tight packing of adjacent hydrophobic lipids and proteins and therefore enhances membrane fluidity (*Fajardo et al., 2011; Seu et al., 2006*). Phosphatidylethanolamine (PE), the second most prominent phospholipid class, restricts movement and thereby decreases membrane fluidity (*Fajardo et al., 2011, Seu et al., 2006).* The smaller ethanolamine head group for once allows tighter packaging and also interacts as hydrogen donor with anionic phosphate-oxygen of adjacent phospholipids (*Fajardo et al., 2011, Seu et al., 2006).*
Under identical conditions for DPH fluorescence anisotropy a not significant tendency toward an increased membrane fluidity was found. This small tendency of the DPH fluorescence anisotropy may be explained by lighter phospholipid packaging mediated by the increased PC content. Therefore, a selective

sensitivity of TMA-DPH but not DPH to changes of the head group region membrane fluidity could be confirmed within own measurements.

The general sensitivity of DPH and TMA-DPH to membrane fluidity changes within our experimental setup was examined by cholesterol depletion using well established methyl-β-cyclodextrine (MβCD) (*Hebbar et al., 2008*; *Zidovetzki & Levitan, 2007*). Decreasing the membrane cholesterol content led to decreased fluorescence anisotropy values corresponding to an increase in membrane fluidity in C6 cells. This effect was more pronounced for DPH than for TMA-DPH. A comparable observation following a similar approach in bovine hippocampal membranes was made by *Pucadyil & Chattopadhyay (2004*). Since cholesterol affects the rotational freedom of PC and sphingomyelin (SM) head group structures (*Ramstedt & Slotte, 2002*) and especially fatty acids (*Chen et al., 1999*) the more pronounced effect seen for DPH is suggested to result at least from immediate local proximity to cholesterol within the hydrophobic core. On the other side TMA-DPH, which is anchored by its polar trimethylamine group, generally shows movement restriction and lower sensitivity to changes in the membrane fluidity, compared to the more lipophilic DPH molecule (*Haertel, 2000; Mulders et al., 1986*).

Although TMA-DPH is supposed to report changes next to the head group region, more recent work identified TMA-DPH to mediate only a minimal positioning change of the DPH fluorophore towards a more external membrane depth (*do Canto et al., 2016; Nelson et al., 2012*). As a result of this minimal difference in membrane depth, TMA-DPH has been suggested to actually being sensitive to at least the glycerol backbone and the upper fatty acids segments and basically report similar changes as DPH (*do Canto et al., 2016; Nelson et al., 2012*). However own results support the idea that these two probes are feasible to distinguish between effects working on lipid head groups (TMA-DPH) from those working more on the lipid core (DPH).

4.2 Adaptive changes within membrane fluidity following chronic incubation of C6 cells with stress hormones

By now, a significant association between stress and depression is well documented (*Tafet et al., 2001*). Therefore, the influence of cortisol and alternatively to adrenaline (due to low stability in aqueous solution) terbutaline (β_2-adrenergic receptor (β_2-AR) specific agonist) and dobutamine (β_1-AR specific agonist) on C6 cell plasma membrane fluidity was investigated. In order to investigate adaptive changes on membrane fluidity C6 cells were incubated for a chronic (6-8 days) time period.

Following chronic incubation with cortisol a dose-dependent membrane fluidity enhancement was determined by decreased fluorescence anisotropy values seen for both DPH and TMA-DPH. Obviously, chronic incubation with cortisol induced adaptive changes in membrane properties, as acute incubation induced an opposite membrane rigidification effect within the head group region of the plasma membrane only, examined by an increased TMA-DPH fluorescence anisotropy. Such a cortisol mediated adaptive enhancement in membrane fluidity, measured by decreased DPH fluorescence anisotropy values was also described in human lymphocytes (*Tolentino et al., 1991*).

Own in parallel performed lipid analyses showed a decreased PC/PE ratio within C6 whole cell lipid extracts following chronic incubation with cortisol. This decrease in PC/PE ratio does however not correlate with the examined membrane fluidity increasing effect, determined by TMA-DPH fluorescence anisotropy. The examined cortisol induced enhancement in membrane fluidity, measured by DPH and TMA-DPH fluorescence anisotropy therefore suggest an underlying increase in membrane core fluidity.

Unfortunately, we found no comparable approach focusing on cortisol mediated adaptive changes in membrane fluidity and associated changes in membrane composition. However, similar studies applying the chemically similar synthetic glucocorticoid dexamethasone (16α-*methyl*-cortisol) have also demonstrated an adaptive enhancement of membrane fluidity in HeLa cells, rat liver cells and intestinal membranes. Within these studies a decreased DPH fluorescence anisotropy seemed to correlate with cell type specific changes including an increase polyunsaturated fatty acid (PUFA) index (*Brasitus et al., 1987;*

Kapitulnik et al., 1986) and a decreased cholesterol/protein ratio (*Johnston & Melnykovych 1980; Johnston et al., 1980*).

A possible selective reduction of PC species, bearing length-chain and highly saturated fatty acid moieties, may theoretically contribute to the examined cortisol induced enhancement of C6 cell membrane fluidity. Mass analysis revealed however a small but nonsignificant decreased choline-D9 incorporation within all main PC-species under investigation. The decreased PC/PE ratio in C6 cells seems therefore to result from a general small decrease in PC synthesis and a suggested increase in PE content. It is therefore highly suggested that cortisol induce a decreased cholesterol content and / or selective changes in fatty acid composition within remaining phospholipid classes associated to induce the examined C6 cell membrane fluidity enhancement.

Neither acute nor chronic incubation with 1 µM terbutaline or dobutamine did affect DPH and TMA-DPH fluorescence anisotropy in C6 cells. Within literature no chronic investigations on membrane fluidity were found.

However a rather acute approach in human adult fibroblasts identified an increased membrane fluidity after 1 h treatment with adrenaline by fluorescence recovery after photobleaching (*Eggl et al., 1986*). Corresponding lipid analysis applying ^{32}P labeling identified a reduced PC and an increased PE synthesis accompanied by a reduced 18:1 fatt acid content of PE (*Eggl et al., 1986*). Rats injected with increasing amounts of norepinephrine for up to 2 weeks showed altered cardiac fatty acid composition of phosphatidylcholine and phosphatidylethanolamine, whereas the other lipid classes were affected only weakly (*Emilsson & Gudbjarnason, 1983*). This included a reduction of PC monounsaturated fatty acids (16:1 and 18:1) (*Emilsson & Gudbjarnason, 1983*). And a partial replacement of linoleic acid (18:2) by arachidonic acid (20:4) in PC and replacement of both 18:2 and 20:4 by docosahexaenoic acid (22:6) in PE (*Gudbjamason & Benediktsdottir, 1996; Emilsson & Gudbjarnason, 1983*). As chronic treatment with terbutaline and dobutamine did not change DPH and TMA-DPH fluorescence anisotropy in C6 cells no corresponding lipid analysis was performed within this work.

4.3 Adaptive changes within membrane fluidity following chronic incubation with antidepressants.

In a following approach antidepressant medication was also tested for a possible adaptive impact on C6 cell membrane fluidity. For this purpose widely used antidepressants of distinct pharmacological mode of action and selectivity were applied. This were for once citalopram a selective serotonin reuptake inhibitor (SSRI), desipramine (DMI) a tricyclic antidepressant (TCA), and the Hypericum perforatum dried extract Ze117. Acute exposure with these antidepressants did not show a direct membrane interacting impact on membrane fluidity determined by unchanged DPH and TMA-DPH fluorescence anisotropy values.

Chronic incubation with citalopram exposed no adaptive changes in C6 cell membrane fluidity, measured by DPH and TMA-DPH fluorescence anisotropy. This result correlated to the in parallel examined unchanged PC/PE ratio and unaffected choline-D9 incorporation rate into main PC species in whole C6 cell lipid extracts.
An unchanged DPH and TMA-DPH fluorescence anisotropy was also described in rat brain plasma membranes after chronic oral citalopram treatment, which was however accompanied by a decreased PE content (*Fišar et al., 2005*).

On the other side chronic incubation with DMI induced an adaptive increase in DPH fluorescence anisotropy in C6 cells, while TMA-DPH fluorescence anisotropy was unaffected. This increase in DPH fluorescence anisotropy stands opposite to the here examined decrease in DPH fluorescence anisotropy after chronic incubation with cortisol. Corresponding lipid analysis showed an unchanged PC/PE ratio, in accordance with the unaffected TMA-DPH fluorescence anisotropy. As the choline-D9 incorporation rate into main PC species was not changed after chronic DMI administration the examined decrease in membrane core fluidity measured by DPH fluorescence anisotropy may be the result of an increased cholesterol content or changed fatty acid profile within other phospholipid classes.
Within a very similar chronic approach applying C6 cells incubated with 10 µM DMI did also not significantly change TMA-DPH fluorescence anisotropy, which shows consistency to own results (*Bürgi, 2001*). However chronic incubation with

10 µM DMI induced a significantly increased PC content and a nonsignificant decreased PE content (*Bürgi, 2001*). This increase in the PC/PE ratio may be the result of the ten times higher DMI concentration, where own observations in C6 cells found only a nonsignificant tendency of an increased PC/PE ratio following chronic treatment with 1 µM DMI. Further own pulse-chase experiments excluded a changed PC content.

However, literature indicates quite controversial effects of DMI on membrane fluidity and the PC/PE content, depending on cell type and experimental approach.

Within ROC-1 cells, a very similar cell type (hybridoma clones between C6 rat glioblastoma cells + rat oligodendrocytes), 4 days of incubation with 5 µM DMI induced decrease in membrane fluidity however especially within superficial layers, which correlated to a significantly decreased PC/PE ratio (*Toplak et al., 1990*). The change in membrane fluidity was measured by increased fluorescence anisotropy values of especially shorter n-(9-anthroyloxy) fatty acid analogues (*Toplak et al., 1990).*

On the other side published in vivo approaches applying DMI long term treatment in rats describe only nonsignificant changes in the PC and PE content in brain homogenates *(Moor et al., 1988)* and in brain plasma membranes (*Fišar et al., 2005*). Parallel DPH and TMA-DPH fluorescence anisotropy measurements in rat brain plasma membranes showed no significant changes in membrane fluidity after chronic oral treatment with DMI (*Fišar et al., 2005*). However, the tendencies toward increasing the membrane fluidity were suggested by the authors to may be modulated at least in part by the cholesterol lowering effect of DMI (*Fišar et al., 2005).*

In contrast to DMI, chronic incubation with Ze117 induced an adaptive membrane rigidification in C6 cells measured by both, DPH and TMA-DPH fluorescence anisotropy. The applied concentration range of 0.01 - 0.05 mg/ml Ze117 already showed a dose-dependent increase in fluorescence anisotropy values of both probes. Remarkably, this effect is opposite to the own described cortisol induced enhancement in C6 cell membrane fluidity, decreasing DPH and TMA-DPH florescence anisotropy.

Within literature no comparable chronic approaches were found. However, 24 h incubation with a Hypericum perforatum extract has also been described to

mediate membrane rigidification in murine microglia (N11) cells, measured by pyrene fluorescence anisotropy (*Kraus et al., 2007*). Within an even shorter approach of only 3 hours after oral administration a decreasing tendency on DPH fluorescence anisotropy was examined in mice brain membranes (*Eckert et al, 2004*). This rather acute in vivo approach, however, may not necessarily be extrapolated on possible chronic long-term changes of membrane fluidity. The in addition performed pyrene measurements also showed only nonsignificant changes, which however showed the opposite direction toward reducing bulk-fluidity (hydrocarbon core) and annular-fluidity (reduced fluidity of lipids close to membrane proteins). The opposite effects within the hydrophobic core seen by DPH and pyrene were discussed by the authors as a result of distinct locations of the fluorescent probes within the membrane hydrophobic core. DPH locates itself parallel to the acyl chains in the center of the lipophilic bilayer leaflets, rather than the core, whereas pyrene is located directly at the terminal of the acyl chains within the bilayer core. The results therefore could be interpreted as decreased lateral diffusion accompanied by an increased rotational movement of the acyl chains (*Eckert et al, 2004*). While these changes in membrane fluidity did not reach significance after Hypericum perforatum extract (*WS 5572*) administration to mice, they did after oral hyperforin administration (*Eckert et al., 2004*).

Available research clearly indicate various bioactive ingredients to contribute to the antidepressant effect of Hypericum perforatum extracts, often in a synergistic manner (*Linde, 2009*). The most interesting components hereby include hyperforin, hypericin and a broad range of flavonoid derivatives (*Butterweck & Schmidt, 2007*; *Paulke et al., 2007*).

Applying HPLC analyses Ze117 was examined for the presence of such compounds and identified hyperforin, hypericin, pseudohypericin and several flavonoids including rutin, hyperoside, quercitrin, isoquercetin, quercetin, biapigenin and amentoflavone. From this spectrum of Ze117 ingredients hyperforin, hypericin, rutin, quercetin, biapigenin, and amentoflavone were chosen and tested for a contributing impact on adaptive C6 cell membrane rigidification.

While no acute changes in DPH and TMA-DPH fluorescence anisotropy were observed, all substances, with the exception of rutin, showed to actually

participate in the adaptive dose-dependent membrane rigidification mediated by Ze117.

The hereby observed membrane fluidity changes can be attributed to substances that all affect DPH fluorescence anisotropy with a varying impact on TMA-DPH fluorescence anisotropy. While hypericin increased DPH and TMA-DPH fluorescence anisotropy values to a similar extend, hyperforin, quercetin and amentoflavone showed to have a comparable lower impact on TMA-DPH fluorescence anisotropy. Biapigenin, which differs from amentoflavone only by the coupling pattern of the two apigenin molecules, affected only DPH fluorescence anisotropy and failed to induce a significant change in TMA-DPH fluorescence anisotropy.

For rutin, which differs from quercetin by an attached rutinose disaccharide and a therefore more hydrophilic character, no significant changes in DPH and TMA-DPH fluorescence anisotropy were found after chronic incubation with 1 µM. However, a possible significant change in membrane fluidity applying a higher rutin concentration, as examined for amentoflavone at a concentration of 1.5 µM, cannot be excluded.

As the described substances show to act primary on the membrane core fluidity the sum effect of these constituents alone may already be responsible for the stronger impact on changing DPH fluorescence anisotropy compared to TMA-DPH following chronic incubation with the Ze117 extract. To the own knowledge this work present an adaptive chronic change in membrane fluidity mediated by constituents of Hypericum perforatum extracts for the first time.

Approaching underlying lipidomic changes after chronic incubation with Ze117 a dose-dependent decrease of the PC/PE ratio was found in C6 whole cell lipid extracts. This dose-dependent decrease of the PC/PE ratio probably contribute to the observed dose-dependent decrease in membrane fluidity, at least within the head group region. This Ze117 mediated impact on the PC/PE ratio is strongly suggested to be the result of changed enzymatic activity either within the biosynthesis or the degradation pathway, or both.

Within this work a PC species specific reduced biosynthesis rate was identified applying parallel choline-D9 pulse-chase experiments, which contribute to the decreased PC/PE ratio in C6 cells after chronic Ze117 treatment.

While the incorporation of cholin-D9 into PC species bearing polyunsaturated fatty acids (18:3, 20:3, 20:4) was found to be unaffected, the de novo biosynthesis of PCs bearing a combination of only saturated and monounsaturated fatty acids was reduced after chronic incubation with Ze117. This affected PC species bearing a combination of 18:1, 16:1, 16:0 and possibly 14:0 fatty acids.

Although, this shift toward an increased PC-PUFA index would be associated with an increased membrane core fluidity, DPH fluorescence anisotropy measurements examined a decreased membrane core fluidity after chronic Ze117 treatment. This membrane fluidity increasing effect of the higher PUFA index is therefore suggested to be compensated at least in part by the tighter membrane packaging mediated by the reduced PC/PE ratio and a stronger intermolecular interaction associated with longer fatty acid chains. Further, the reduction of cis-configurated monounsaturated palmitoleic acid (16:1) and oleic acid (18:1), which bended tails disrupt tight packing and interaction of fatty acids, can also be associated with a reduced membrane fluidity (*Vance & Vance, 2008; Pilch et al., 1980; Kitagawa et al. 1985*).

During PC de novo biosynthesis fatty acids incorporated into the *sn-1* and *sn-2* position are generally saturated and monounsaturated fatty acids (*Robichaud et al., 2013*). The hereby converted diacylglycerol (DAG) molecule results from the interplay of different glycerol-3-phosphate acyltransferases (GPATs) and lysophospholipid acyltransferases (LPLATs). Rapid phospholipid remodulation and incorporation of PUFAs at the *sn-2* position occurs after de novo biosynthesis, characterized by deacylation and subsequent reacylation catalyzed by a phospholipase A_2 (PLA_2) and a LPLAT (*Farooqui et al.,* 2000; Shindou & Shimizu, 2009). The fatty acid released from the sn-2 position become again activated by a acyl-CoA synthetase (ACS) to produce acyl-CoA (*Robichaud et al., 2013*).

As Ze117 mediates selective reduced cholin-D9 incorporation into PC species bearing saturated and monounsaturated acids but not PC species bearing a PUFA it may be suggested that possibly de-novo synthesis of PC is reduced in general while reacylation at the *sn-2* position with PUFA is kept constant.

However the interplay between phospholipid *de novo* and remodeling pathway is complex and poorly understood (*Butler & Mallampalli, 2010*). Overexpression

of lysophatidylcholine acyltransferase 1 (LPCAT1) has for example been reported to induce increased degradation of CPT1 (cholinephosphotransferase 1), which catalyzes the final step for the PC *de novo* synthesis (*Butler & Mallampalli, 2010*). And hypericin mediated inhibition of protein kinase C (PKC), which increases catalytic PLA_2-activity by phosphorylation, was described to inhibit PC biosynthesis in U937 cells (*Chu, 1994; Nemenoff et al., 1993*).

Several subtypes of GPAT, LPLAT, PLA_2, and ACS with characteristic substrate specificities have been discovered and their differential expression is suggested to regulate tissue specific diversity of phospholipid molecular species (*Robichaud et al., 2013; Shindou et al., 2015; Harayama et al., 2014*).

Interestingly hyperforin has been described to mediate enhanced cytosolic phospholipase A_2 ($cPLA_2$) activity in human platelets, which shows to prefer PC over PE (*Hoffmann et al., 2010*). Further $cPLA_2$ cleaves preferentially long and polyunsaturated fatty acids, showing the highest affinity for arachidonic acid (20:4) containing phospholipids (*Kramer & Sarp, 1997; Hoffmann et al., 2010*).

On the other side quercetin and amentoflavone have been reported to show an inhibitory effect on the selective type II phospholipase A_2 (PLA_2-type II) (*Patočka, 2003; Lindahl & Tagesson 1997; Lindhal & Tagesson, 1993*). The PLA_2-type II is described to show a strong preference for negatively charged phospholipids including PE and PS, releasing a variety of unsaturated fatty acids (*Diez et al., 1994; Freed et al., 1997; Snitko et al., 1997*).

In association to own results in C6 cells, those constituents which showed a chronic impact on membrane fluidity are highly suggested to modulate membrane lipid composition. The observed reduced synthesis of PC species bearing saturated and monounsaturated fatty acids can be suggested to result from down-regulation or inhibition of enzymes catalyzing the de-novo pathway. A theoretical hyperforin mediated enhanced hydrolysis of PC species bearing PUFA may be compensated by a generally increased turnover including an enhanced reacylation with PUFAs, keeping the amount of PUFA bearing PC species constant. This could be the result of enhanced acylation with a lysophosphocholine acyltransferase (LPCAT) like LPCAT2 which prefers 20:4 acyl-CoAs as substrate (*Shindou & Shimizu, 2009*).

4.4 Conclusion and Outlook

The presented findings regarding fluorescence anisotropy measurements applying DPH and TMA-DPH identified a membrane fluidity increasing effect in C6 cells stressed by chronic cortisol incubation. An opposite effect was found after chronic Ze117 treatment, which was identified to be mediated at least by the constituents hypericin, hyperforin, quercetin, amentoflavone and biapigenin. The tricyclic antidepressant DMI also showed to expose an adaptive decrease in membrane fluidity, however only in the membrane core as measured by increased DPH fluorescence anisotropy. Since membrane fluidity has a regulatory impact on membrane-associated receptor functioning, it can be suggested that the cortisol mediated adaptive changes in membrane fluidity contribute to the altered monoamine receptor signaling as described within depression. As Ze117 and in part DMI, showed an opposite adaptive effect compared to chronic cortisol treatment in C6 cells it may be assumed that this antidepressants may have a “normalizing” effect on the membrane fluidity of "stressed" cells and possibly on the functioning of membrane-associated receptors.

In contrast to cortisol and DMI, chronic Ze117 incubation mediated changes in membrane fluidity at least in part by modulating the PC pool and PC/PE ratio. The hereby examined reduced synthesis of PC species bearing saturated and monounsaturated fatty acids may result from down-regulation or inhibition of enzymes catalyzing the de-novo pathway. This enzymes include choline kinase (CK), CTP:phosphocholine cytidylyltransferase (CCT) which catalyzes the rate-limiting enzymatic step, and CDP-choline:1,2-diacylglycerol cholinephosphotransferase (CPT) which is mainly regulated by DAG availability (*Gibellini & Smith, 2010*). Whereby DAG generation could also be modulated by downregulation of specific LPLATs and GPATs, like the 16:0 acyl-CoA preferring GPAT1 (*Shindou & Shimizu, 2009*). A theoretically reduced activity of LPCAT1 and LPCAT4, which participate within the de-novo and the remodeling pathway, or limitation of their corresponding acyl-CoA substrate availability could also explain the reduced production of PC species bearing saturated and monounsaturated fatty acids. Hereby LPCAT1 has been reported to prefer saturated 16:0 acyl-CoAs (*Butler & Mallampalli, 2010; Harayama et al., 2014*), but also 18:1 acyl-CoA (*Shindou & Shimizu, 2009*) as a donor and 1-myristoyl

(14:0) or 1-palmitoyl (16:0) -lysoPC as an acceptor (*Butler & Mallampalli, 2010*). LPCAT4 (also named MBOAT2) plays a catalytic role with a preference for 16:1- and 18:1 acyl-CoA within the PC synthesis (*Kurabe et al., 2013; Harayama et al., 2014; Hishikawa et al., 2008; Shindou & Shimizu, 2009*).

It must be assumed that several bioactive ingredients of Ze117 participate in the modulation of the phospholipid composition by various mechanisms targeting at least the PC de-novo synthesis and the fatty acid remodeling pathway. Within this context several specific PLA_2 activity regulating effects have been described in literature for at least hyperforin, hypericin, quercetin and amentoflavone (*Hoffmann et al., 2010; Chu, 1994; Patočka, 2003; Lindahl & Tagesson 1997*). Within future approaches the impact of Ze117 and individual constituents on de-novo catalyzing enzymes as well as their interplay with selective subtypes of GPAT, LPLAT, PLA_2, and ACS, with characteristic substrate specificities, may be considered.

5 References

Andrade, C., & Rao, N. (2010). How antidepressant drugs act: A primer on neuroplasticity as the eventual mediator of antidepressant efficacy. *Indian Journal of Psychiatry*, *52*(4), 378–386.

Aricha, B., Fishov, I., Cohen, Z., Sikron, N., Khozin-Goldberg, I., Dagan, R., et al., (2004). Differences in Membrane Fluidity and Fatty Acid Composition between Phenotypic Variants of Streptococcus pneumoniae. *Journal of Bacteriology*, *186*(14), 4638–4644.

Berton, O., & Nestler, E. J. (2006). New approaches to antidepressant drug discovery: Beyond monoamines. *Nature Reviews Neuroscience*, *7*(2), 137–151.

Brasitus, T. a, Dudeja, P. K., Dahiya, R., & Halline, A. (1987). Dexamethasone-induced alterations in lipid composition and fluidity of rat proximal-small-intestinal brush-border membranes. *The Biochemical Journal*, *248*(2), 455–461.

Bürgi, S. C. (2001). Antidepressiva-induzierte ß-Adrenozeptor-Down regulation. *Doctoral Dissertation, ETH Zurich*.

Butler, P. L., & Mallampalli, R. K. (2010). Cross-talk between remodeling and de novo pathways maintains phospholipid balance through ubiquitination. *Journal of Biological Chemistry*, *285*(9), 6246–6258.

Butterweck, V., & Schmidt, M. (2007). St. John's wort: Role of active compounds for its mechanism of action and efficacy. *Wiener Medizinische Wochenschrift*, *157*(13–14), 356–361.

Charney, D. S., & Manji, H. K. (2004). Life stress, genes, and depression: multiple pathways lead to increased risk and new opportunities for intervention. *Science's STKE : Signal Transduction Knowledge Environment*, *2004*(*225*),re5 1–11.

Chen, Q., Amaral, J., Biancani, P., & Behar, J. (1999). Excess membrane cholesterol alters human gallbladder muscle contractility and membrane fluidity. *Gastroenterology*, *116*(3), 678–685.

Chrousos, G. P. (2009). Stress and disorders of the stress system. *Nature Reviews Endocrinology*, *5*(7), 374–381.

Chu, A. J. (1994). Differential Regulations of Biosynthesis in U937 Cells by Inhibitors of Protein and Tyrosine. *International Journal of Biocemistry*, *26*(2), 189–193.

Concerto, C., Boo, H., Hu, C., Sandilya, P., Krish, A., Chusid, E., et al., (2018). Hypericum perforatum extract modulates cortical plasticity in humans. *Psychopharmacology*, *235*(1), 145–153.

Davis, M. T., Holmes, S. E., Pietrzak, R. H., & Esterlis, I. (2017). Neurobiology of Chronic Stress-Related Psychiatric Disorders. *Chronic Stress*, *1*, 1–21.

De Kloet, E. R., Joëls, M., & Holsboer, F. (2005). Stress and the brain: From adaptation to disease. *Nature Reviews Neuroscience*, *6*(6), 463–475.

Deliconstantinos, G. (1985). Cortisol effect on (Na^++K^+)-stimulated ATPase activity and on bilayer fluidity of dog brain synaptosomal plasma membranes. *Neurochemical Research*, *10*(12), 1605–1613.

DGPPN, BÄK, KBV, AWMF, AkdÄ, BPtK, et al., (2015). S3-Leitlinie / Nationale VersorgungsLeitlinie Unipolare Depression - Langfassung. *Ärztliches Zentrum Für Qualität Der Medizin*, *2*(1).

Diez, E., Chilton, F. H., Stroup, G., Mayer, R. J., Winkler, J. D., & Fonteh, A. N. (1994). Fatty acid and phospholipid selectivity of different phospholipase A2 enzymes studied by using a mammalian membrane as substrate. *The Biochemical Journal*, *301*(Pt 3), 721–726.

Dindia, L., Murray, J., Faught, E., Davis, T. L., Leonenko, Z., & Vijayan, M. M. (2012). Novel Nongenomic Signaling by Glucocorticoid May Involve Changes to Liver Membrane Order in Rainbow Trout. *PLoS ONE*, *7*(10).

do Canto, A. M. T. M., Robalo, J. R., Santos, P. D., Carvalho, A. J. P., Ramalho, J. P. P., & Loura, L. M. S. (2016). Diphenylhexatriene membrane probes DPH and TMA-DPH: A comparative molecular dynamics simulation study. *Biochimica et Biophysica Acta - Biomembranes*, *1858*(11), 2647–2661.

Duman, R. S., Aghajanian, G. K., Sanacora, G., & Krystal, J. H. (2016). Synaptic plasticity and depression: New insights from stress and rapid-acting antidepressants. *Nature Medicine*, *22*(3), 238–249.

Dyall, S. C. (2015). Long-chain omega-3 fatty acids and the brain: A review of the independent and shared effects of EPA, DPA and DHA. *Frontiers in Aging Neuroscience*, *7*(52), 1–15.

Eckert, G. P., Keller, J. H., Jourdan, C., Karas, M., Volmer, D. A., Schubert-Zsilavecz, M., & Müller, W. E. (2004). Hyperforin modifies neuronal membrane properties in vivo. *Neuroscience Letters*, *367*(2), 139–143.

Eggl, P., Wirthensohn, K., & Hisch, H. (1986). Effect of hormones on phospholipid metabolism in human cultured fibroblasts. *Biocimica et Biophysica Acta*, *862*(2), 399–406.

Emilsson, A., & Gudbjarnason, S. (1983). Reversible alterations in fatty acid profile of glycerophospholipids. *Biochimica et Biophysica Acta (BBA)*, *750*(1), 1–6.

Ernst, E. (2007). Herbal remedies for depression and anxiety. *Advances in Psychiatric Treatment*, *13*(4), 312–316.

Fagone, P., & Jackowski, S. (2013). Phosphatidylcholine and the CDP-choline cycle. *Biochimica et Biophysica Acta - Molecular and Cell Biology of Lipids*, *1831*(3), 523–532.

Fajardo, V. A., McMeekin, L., & Leblanc, P. J. (2011). Influence of phospholipid species on membrane fluidity: A meta-analysis for a novel phospholipid fluidity index. *Journal of Membrane Biology*, *244*(2), 97–103.

Faria, R., Santana, M. M., Aveleira, C. A., Simões, C., Maciel, E., Melo, T., et al., (2014). Alterations in phospholipidomic profile in the brain of mouse model of depression induced by chronic unpredictable stress. *Neuroscience*, *273*, 1–11.

Farooqui, A. A., Horrocks, L. A., & Farooqui, T. (2000). Glycerophospholipids in brain: Their metabolism, incorporation into membranes, functions, and involvement in neurological disorders. *Chemistry and Physics of Lipids*, *106*(1), 1–29.

Fava, M., & Kendler, K. S. (2000). Major Depressive Disorder Review. *Neuron*, *28*(2), 335–341.

Fernandes, M. F., Mutch, D. M., & Leri, F. (2017). The relationship between fatty acids and different depression-related brain regions, and their potential role as biomarkers of response to antidepressants. *Nutrients*, *9*(3), 298.

Fernstrom, J. D. (1994). 9. Stress and monoamine neurons in the brain. *Food Components to Enhance Performance*, 161–175.

Filburn, C. R. (2000). Dietary Supplementation with Phospholipids and Docosahexaenoic Acid for Age-Related Cognitive Impairment. *The Journal of the American Nutraceutical Association, 3*(3), 45–55.

Fišar, Z., Anders, M., Tvrzická, E., & Staňková, B. (2005). Effect of long-term administration of antidepressants on the lipid composition of brain plasma membranes. *General Physiology and Biophysics*, *24*(2), 221–236.

Floyd, K., Mikkelson, A. C., Hesse, C., & Pauley, P. M. (2007). Affectionate writing reduces total cholesterol: Two randomized, controlled trials. *Human Communication Research*, *33*(2), 119–142.

Fraňová, M., Repáková, J., Čapková, P., Holopainen, J. M., & Vattulainen, L. (2010). Effects of DPH on DPPC-Cholesterol membranes with varying concentrations of cholesterol: From local perturbations to limitations in fluorescence anisotropy experiments. *Journal of Physical Chemistry B*, *114*(8), 2704–2711.

Freed, K., Moses, E., Brennecke, S., & Rice, G. (1997). Differential expression of type II, IV and cytosolic PLA2 messenger RNA in human intrauterine tissues at term. *Molecular Human Reproduction*, *3*(6), 493–499.

Frodl, T., & O'Keane, V. (2013). How does the brain deal with cumulative stress? A review with focus on developmental stress, HPA axis function and hippocampal structure in humans. *Neurobiology of Disease*, *52*, 24–37.

Gibellini, F., & Smith, T. K. (2010). The Kennedy pathway-de novo synthesis of phosphatidylethanolamine and phosphatidylcholine. *IUBMB Life*, *62*(6), 414–428.

Gudbjamason, S., & Benediktsdottir, V. E. (1996). Regulation of ß-adrenoceptor properties and the lipid milieu in heart muscle membranes during stress. *Molecular and Cellular Biochemistry*, *163–164*(1), 137–143.

Gunnar, M., & Quevedo, K. (2007). The Neurobiology of Stress and Development. *Annual Review of Psychology*, *58*, 145–173.

Harayama, T., Eto, M., Shindou, H., Kita, Y., Otsubo, E., Hishikawa, D., et al., (2014). Lysophospholipid acyltransferases mediate phosphatidylcholine diversification to achieve the physical properties required in vivo. *Cell Metabolism*, *20*(2), 295–305.

Härtel, S. (2000). Quantifizierung von Strukturen, Kinetik und Dynamik nekrobiologischer Prozesse mit Hilfe bildverarbeitender konfokaler Fluoreszenzmikroskopie. *Doctoral Dissertation, University of Bremen, Germany*.

Hay, S. I. (2017). Global, regional, and national incidence, prevalence, and years lived with disability for 328 diseases and injuries for 195 countries, 1990-2016: A systematic analysis for the Global Burden of Disease Study 2016. *The Lancet*, *390*(10100), 1211–1259.

Hebbar, S., Lee, E., Manna, M., Steinert, S., Kumar, G. S., Wenk, M., et al., (2008). A fluorescent sphingolipid binding domain peptide probe interacts with sphingolipids and cholesterol-dependent raft domains. *Journal of Lipid Research*, *49*(5), 1077–1089.

Hindmarch, I. (2001). Expanding the horizons of depression: Beyond the monoamine hypothesis. *Human Psychopharmacology*, *16*(3), 203–218.

Hishikawa, D., Shindou, H., Kobayashi, S., Nakanishi, H., Taguchi, R., & Shimizu, T. (2008). Discovery of a lysophospholipid acyltransferase family essential for membrane asymmetry and diversity. *Proceedings of the National Academy of Sciences*, *105*(8), 2830–2835.

Hoffmann, M., Lopez, J. J., Pergola, C., Feisst, C., Pawelczik, S., Jakobsson, P. J., et al., (2010). Hyperforin induces Ca2+-independent arachidonic acid release in human platelets by facilitating cytosolic phospholipase A2activation through select phospholipid interactions. *Biochimica et Biophysica Acta - Molecular and Cell Biology of Lipids*, *1801*(4), 462–472.

Jakobs, D., Hage-Hülsmann, A., Prenner, L., Kolb, C., Weiser, D., & Häberlein, H. (2013). Downregulation of β1-adrenergic receptors in rat C6 glioblastoma cells by hyperforin and hyperoside from St John's wort. *Journal of Pharmacy and Pharmacology*, *65*(6), 907–915.

Jamil, H., & Vance, D. E. (1990). Head-group specificity for feedback regulation of CTP:phosphocholine cytidylyltransferase. *Biochem J*, *270*(3), 749–754.

Joca, S. R. L., Ferreira, F. R., & Guimarães, F. S. (2007). Modulation of stress consequences by hippocampal monoaminergic, glutamatergic and nitrergic neurotransmitter systems. *Stress*, *10*(3), 227–249.

Johnston, D., Matthews, E. R., & Melnykovych, G. (1980). Glucocorticoid effects on lipid metabolism in hela cells: Inhibition of cholesterol synthesis and increased sphingomyelin synthesis. *Endocrinology*, *107*(5), 1482–1488.

Johnston, D., & Melnykovych, G. (1980). Effects of dexamethasone on the fluorescence polarization of diphenylhexatriene in HeLa cells. *Biochimica et Biophysica Acta (BBA)- Biomembranes*, *596*(2), 320–324.

Jow, G. M., Yang, T. T., & Chen, C. L. (2006). Leptin and cholesterol levels are low in major depressive disorder, but high in schizophrenia. *Journal of Affective Disorders*, *90*(1), 21–27.

Kapitulnik, J., Weil, E., & Rabinowitz, R. (1986). Glucocorticoids increase the fluidity of the fetal-rat liver microsomal membrane in the perinatal period. *The Biochemical Journal*, *239*(1), 41–45.

Kidd, P. M. (2007). Omega -3 DHA and EPA for Cognition , Behavior, and Mood : Clinical Findings and Structural- Functional Synergies with Cell Membrane Phospholipids. *Alternative Medicine Review*, *12*(3), 207–227.

Kidd, P. M. (2004). Bipolar disorder as cell membrane dysfunction. Progress toward integrative management. *Alternative Medicine Review*, *9*(2), 107–135.

Kitagawa, S., Junko, E., & Kametani, F. (1985). Measurement of fluorescence polarization . Fluo- Effects of long-chain cis-unsaturated fatty acids on platelet aggregation. *Biochimica et Biophysica Acta (BBA)-Biomembranes*, *818*(3), 391–397.

Kramer, R. M., & Sharp, J. D. (1997). Structure, function and regulation of Ca2+-sensitive cytosolic phospholipase A2 (cPLA2). *FEBS Letters*, *410*(1), 49–53.

Kraus, B., Wolff, H., Heilmann, J., & Elstner, E. F. (2007). Influence of Hypericum perforatum extract and its single compounds on amyloid-β mediated toxicity in microglial cells. *Life Sciences*, *81*(11), 884–894.

Kurabe, N., Hayasaka, T., Ogawa, M., Masaki, N., Ide, Y., Waki, M., et al., (2013). Accumulated phosphatidylcholine (16:0/16:1) in human colorectal cancer; possible involvement of LPCAT4. *Cancer Science*, *104*(10), 1295–1302.

Kyrou, I., & Tsigos, C. (2007). Stress mechanisms and metabolic complications. *Hormone and Metabolic Research*, *39*(6), 430–438.

Lakowicz, J. R. (2006). *Principles of Fluorescence Spectroscopy. Springer, New York, USA, 3rd Edn,*

Lee, S., Jeong, J., Kwak, Y., & Park, S. K. (2010). Depression research: Where are we now? *Molecular Brain*, *3*(1), 8.

Li, Y., Holzwarth, J. F., & Bohne, C. (2000). Aggregation dynamics of sodium taurodeoxycholate and sodium deoxycholate. *Langmuir*, *16*(4), 2038–2041.

Lindahl, M., & Tagesson, C. (1997). Flavonoids as phospholipase A_2 inhibitors : importance of their structure for selective inhibition of group II phospholipase A_2 . *Inflammation*, *21*(3), 347–356.

Lindahl, M., & Tagesson, C. (1993). Selective inhibition of group II phospholipase A_2 by quercetin. *Inflammation*, *17*(5), 573–582.

Linde, K. (2009). St. John's Wort - An overview. *Complementary Medicine Research*, *16*(3), 146–155.

Logan, A. C. (2003). Neurobehavioral aspects of omega-3 fatty acids: possible mechanisms and therapeutic value in major depression. *Alternative Medicine Review, 8*(4), 410–425.

Los, D. A., & Murata, N. (2004). Membrane fluidity and its roles in the perception of environmental signals. *Biochimica et Biophysica Acta - Biomembranes*, *1666*(1), 142–157.

Loura, L. M. S., & Ramalho, J. P. P. (2011). Recent developments in molecular dynamics simulations of fluorescent membrane probes. *Molecules*, *16*(7), 5437–5452.

Magalhães, R., Bourgin, J., Boumezbeur, F., Marques, P., Bottlaender, M., Poupon, C., et al., (2017). White matter changes in microstructure associated with a maladaptive response to stress in rats. *Translational Psychiatry*, *7*(1), e1009.

Marcinko, D., Martinac, M., Karlović, D., Filipcić, I., Loncar, C., Pivac, N., & Jakovljević, M. (2005). Are there differences in serum cholesterol and cortisol concentrations between violent and non-violent schizophrenic male suicide attempters? *Collegium Antropologicum*, *29*(1), 153–157

Massart, R., Mongeau, R., & Lanfumey, L. (2012). Beyond the monoaminergic hypothesis: neuroplasticity and epigenetic changes in a transgenic mouse model of depression. *Philosophical Transactions of the Royal Society B: Biological Sciences*, *367*(1601), 2485–2494.

Mischoulon, D., & Rosenbaum, J. F. (2008). Natural Medications for Psychiatric Disorders: Considering the Alternatives. *Lippincott Williams & Wilkins.*

Mitchell, T. W., Ekroos, K., Blanksby, S. J., Hulbert, A. J., & Else, P. L. (2007). Differences in membrane acyl phospholipid composition between an endothermic mammal and an ectothermic reptile are not limited to any phospholipid class. *Journal of Experimental Biology*, *210*(19), 3440–3450.

Moor, M., Honegger, U. E., & Wiesmann, U. N. (1988). Organspecific, qualitative changes in the phospholipid composition of rats after chronic administration of the antidepressant drug desipramine. *Biochemical Pharmacology*, *37*(10), 2035–2039.

Mulders, F., Langen, H. Van, Ginkel, G. Van, & Levine, Y. K. (1986). The static and dynamic behaviour of fluorescent probe molecules in lipid bilayers. *Biochimica et Biophysica Acta (BBA)- Biomembranes*, *859*(2), 209–218.

Nelson, S. C., Neeley, S. K., Melonakos, E. D., Bell, J. D., & Busath, D. D. (2012). Fluorescence anisotropy of diphenylhexatriene and its cationic Trimethylamino derivative in liquid dipalmitoylphosphatidylcholine liposomes: Opposing responses to isoflurane. *BMC Biophysics*, *5*(1), 5.

Nemenoff, R. A., Winitz, S., Qian, N. X., Van Putten, V., Johnson, G. L., & Heasley, L. E. (1993). Phosphorylation and activation of a high molecular weight form of phospholipase A_2 by p42 microtubule-associated protein 2 kinase and protein kinase C. *Journal of Biological Chemistry*, *268*(3), 1960–1964.

Neu, J., Ozaki, C. K., & Angelides, K. J. (1986). Glucocorticoid-mediated alteration of fluidity of brush border membrane in rat small intestine. *Pediatric Research*, *20*(1), 79–82.

Ohvo-Rekilä, H., Ramstedt, B., Leppimäki, P., & Peter Slotte, J. (2002). Cholesterol interactions with phospholipids in membranes. *Progress in Lipid Research*, *41*(1), 66–97.

Oliveira, T. G., Chan, R. B., Bravo, F. V., Miranda, A., Silva, R. R., Zhou, B., et al., (2016). The impact of chronic stress on the rat brain lipidome. *Molecular Psychiatry*, *21*(1), 80–88.

Papakostas, G. I., Öngür, D., Iosifescu, D. V., Mischoulon, D., & Fava, M. (2004). Cholesterol in mood and anxiety disorders: Review of the literature and new hypotheses. *European Neuropsychopharmacology*, *14*(2), 135–142.

Patočka J. (2003). The chemistry, pharmacology, and toxicology of the biologically active constituents of the herb Hypericum perforatum L. *Journal of Applied Biomedicine*, *1*(2), 61–70.

Patrick, R. P., & Ames, B. N. (2015). Vitamin D and the omega-3 fatty acids control serotonin synthesis and action, part 2: Relevance for ADHD, bipolar disorder, schizophrenia, and impulsive behavior. *The FASEB Journal*, *29*(6), 2207–2222.

Paulke, A., Nöldner, M., Schubert-Zsilavecz, M., & Wurglics, M. (2008). St. John's wort flavonoids and their metabolites show antidepressant activity and accumulate in brain after multiple oral doses. *Pharmazie-An International Journal of Pharmaceutical Sciences*, *63*(4), 296–302.

Peet, M., & Stokes, C. (2005). Omega-3 Fatty Acids in the Treatment of Psychiatric Disorders. *Drugs*, *65*(8), 1051–1059.

Pilch, P. F., Thompson, P. A., & Czech, M. P. (1980). Coordinate modulation of D-glucose transport activity and bilayer fluidity in plasma membranes derived from control and insulin-treated adipocytes. *Proceedings of the National Academy of Sciences*, *77*(2), 915–918.

Pucadyil, T. J., & Chattopadhyay, A. (2004). Cholesterol modulates ligand binding and G-protein coupling to serotonin1A receptors from bovine hippocampus. *Biochimica et Biophysica Acta - Biomembranes*, *1663*(1), 188–200.

Rabasa, C., & Dickson, S. L. (2016). Impact of stress on metabolism and energy balance. *Current Opinion in Behavioral Sciences*, *9*, 71–77.

Ramstedt, B., & Slotte, J. P. (2002). Membrane properties of sphingomyelins. *FEBS Letters*, *531*(1), 33–37.

Reddy, M. (2010). Depression: The disorder and the burden. *Indian Journal of Psychological Medicine*, *32*(1), 1.

Repáková, J., Holopainen, J. M., Morrow, M. R., McDonald, M. C., Čapková, P., & Vattulainen, I. (2005). Influence of DPH on the structure and dynamics of a DPPC bilayer. *Biophysical Journal*, *88*(5), 3398–3410.

Robichaud, P. P., Boulay, K., Munganyiki, J. É., & Surette, M. E. (2013). Fatty acid remodeling in cellular glycerophospholipids following the activation of human T cells. *Journal of Lipid Research*, *54*(10), 2665–2677.

Sarris, J. (2011). Clinical depression: an evidence-based integrative complementary medicine treatment model. *Alternative Therapies in Health and Medicine*, *17*(4), 26–37.

Schwarz, E., Prabakaran, S., Whitfield, P., Major, H., Leweke, F. M., Koethe, D., et al., (2008). High throughput lipidomic profiling of schizophrenia and bipolar disorder brain tissue reveals alterations of free fatty acids, phosphatidylcholines, and ceramides. *Journal of Proteome Research*, *7*(10), 4266–4277.

Seu, K. J., Cambrea, L. R., Everly, R. M., & Hovis, J. S. (2006). Influence of lipid chemistry on membrane fluidity: Tail and headgroup interactions. *Biophysical Journal*, *91*(10), 3727–3735.

Shindou, H., Harayama, T., & Hishikawa, D. (2015). Chapter: Lysophospholipid Acyltransferases. In Yokomizo, T. & Murakami, M. (Eds.), *Bioactive Lipid Mediators. Current Reviews and Protocols* (pp. 3–21). Springer Japan.

Shindou, H., & Shimizu, T. (2009). Acyl-CoA:lysophospholipid acyltransferases. *Journal of Biological Chemistry*, *284*(1), 1–5.

Snitko, Y., Yoon, E. T., & Cho, W. (1997). High specificity of human secretory class II phospholipase A2 for phosphatidic acid. *Biochem J*, *321*(Pt 3), 737–741.

Sumbilla, C., & Lakowicz, J. R. (1983). Evidence for normal fibroblast cell membranes from individuals with Huntington´s disease: A fluorescence probe study. *Journal of Neurological Sciences*, *62*(1–3), 23–40.

Tafet, G. E., & Bernardini, R. (2003). Psychoneuroendocrinological links between chronic stress and depression. *Progress in Neuro-Psychopharmacology and Biological Psychiatry*, *27*(6), 893–903.

Tolentino, M. V., Sarasua, M. M., Hill, O. A., Wentworth, D. B., Franceschi, D., & Fratianne, R. B. (1991). Peripheral lymphocyte membrane fluidity after thermal injury. *The Journal of Burn Care & Rehabilitation*, *12*(6), 498–504.

Toplak, H., Zuehlke, R., Loidl, S., Hermetter, A., Honegger, U. E., & Wiesmann, U. N. (1990). Single and multiple desipramine exposures of cultured cells. Changes in cellular anisotropy and in lipid composition of whole cells and of plasma membranes. *Biochemical Pharmacology*, *39*(9), 1437–1443.

Tsigos, C., & Chrousos, G. P. (2002). Hypothalamic – pituitary – adrenal axis, neuroendocrine factors and stress. *Journal of Psychosomatic Research, 53*(4), 865–871.

van Bodegom, M., Homberg, J. R., & Henckens, M. J. A. G. (2017). Modulation of the Hypothalamic-Pituitary-Adrenal Axis by Early Life Stress Exposure. *Frontiers in Cellular Neuroscience*, *11*, 87.

Van Meer, G. (2005). Cellular lipidomics. *The EMBO Journal*, *24*(18), 3159–3165.

Vance, D. E., & Vance, J. E. (2008). *Biochemistry of Lipids, Lipoproteins and Membranes*. *Elsevier*. *5th Edn.*

Weisbuch, M., Seery, M. D., Ambady, N., & Blascovich, J. (2009). On the Correspondence between Physiological and Nonverbal Responses: Nonverbal Behavior Accompanying Challenge and Threat. *Journal of Nonverbal Behavior*, *33*(2), 141–148.

Weiser, M. J., Butt, C. M., & Mohajeri, M. H. (2016). Docosahexaenoic acid and cognition throughout the lifespan. *Nutrients*, *8*(2), 99.

Whiskey, E., Werneke, U., & Taylor, D. (2001). A systematic review and meta-analyis of Hypericum perforatum in depression: A comprehensive clinical review. *International Clinical Psychopharmacology*, *16*(5), 239–252

Wong, M.-L., & Licinio, J. (2001). Research and treatment approaches to depression. *Nature Reviews Neuroscience*, *2*(5), 343–351.

Yehuda, S., Rabinovitz, S., Carasso, R. L., & Mostofsky, D. I. (2000). Fatty acid mixture counters stress changes in cortisol, cholesterol, and impair learning. *Int J Neurosci*, *101*(1–4), 73–87.

Zidovetzki, R., & Levitan, I. (2007). Use of cyclodextrins to manipulate plasma membrane cholesterol content: evidence, misconceptions and control strategies. *Biochimica et Biophysica Acta (BBA) - Biomembranes*, *1768*(6), 1311–1324.

6 Appendix

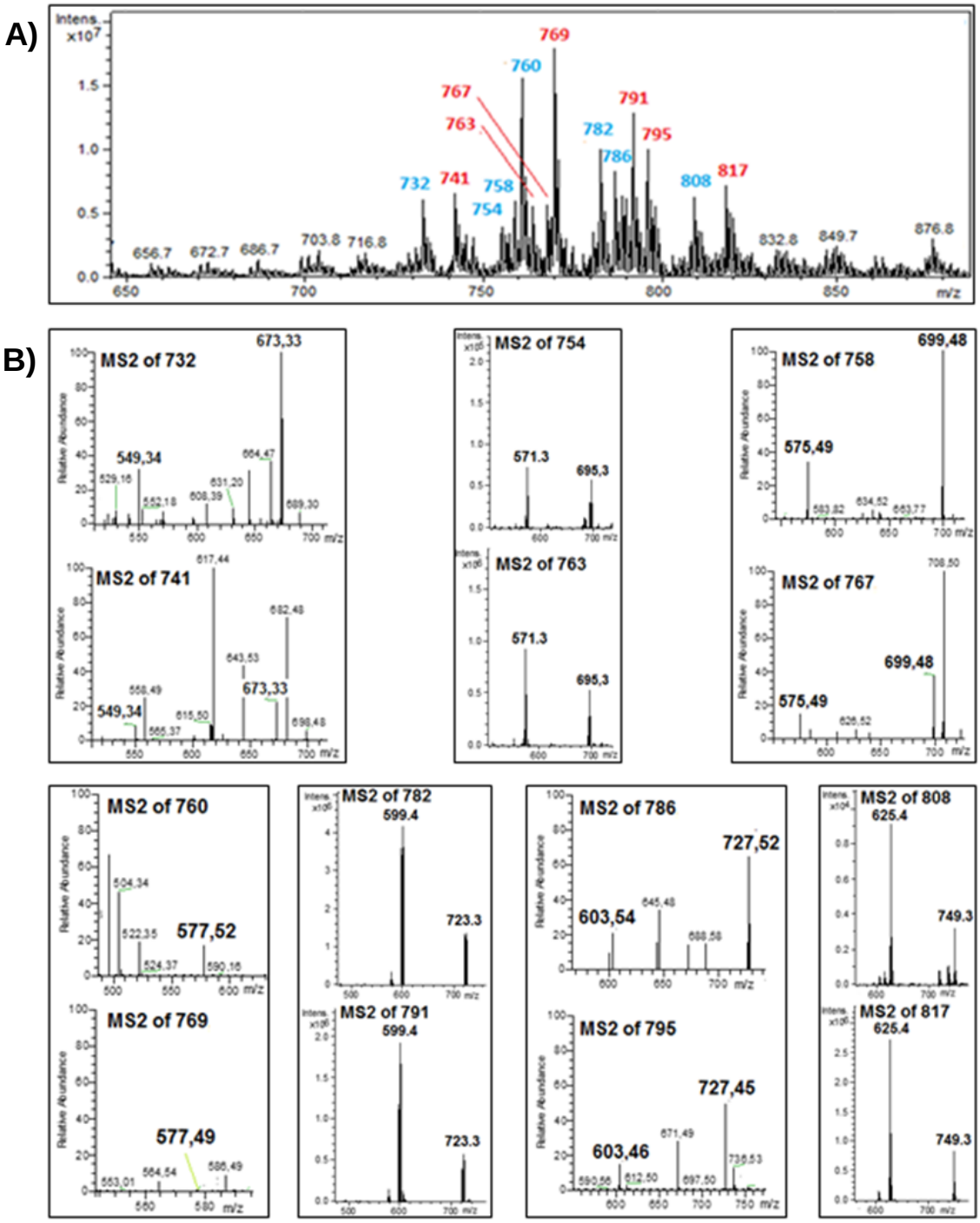

Figure 6.1: MS spectra of PC-pairs identification in whole cell lipid extracts after choline-D9 exposure to C6 cells. The incorporation of choline-D9 into PC via the de-novo biosynthesis pathway results in the appearance of deuterated PC derivatives (**red**) of corresponding natural occurring PC species (**blue**)(A). Each pair with the mass shift of 9 was proven to represent the deuterated derivative and the natural occurring PC species by forming at least an identical DAG-like fragment after MS2 fragmentation (B).

Fatty acid identification applying chloride adducts

Fatty acid identification applying acetate adducts

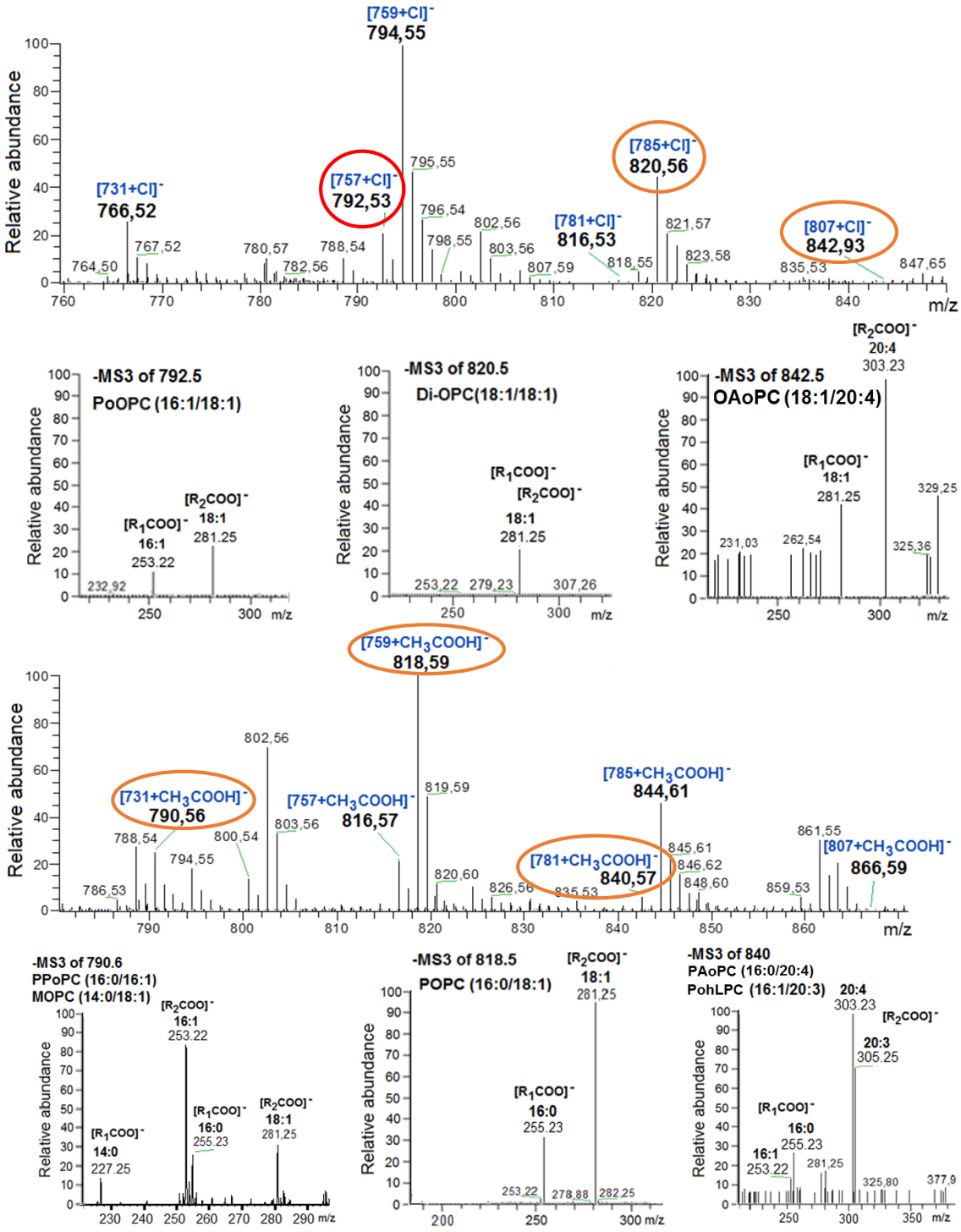

Figure 6.2: Negative mode MS spectra of PC species identification applying anionic PC adducts. Main PC species previously investigated at positive mode as $[M+H]^+$ cations are detected within the negative mode as anionic chloride $[M+Cl]^-$ or acetate $[M+CH_3COO]^-$ adduct. Corresponding MS3 fragmentation results in the identification of attached fatty acids. The sn-2 fatty acid fragment $[R_2COO]^-$ is distinguished from the sn-1 fatty acid fragment $[R_1COO]^-$ due to it appears with a higher abundancy.

Eidesstattliche Erklärung

Hiermit versichere ich, Nelli Keksel, dass ich die vorliegende Arbeit selbstständig angefertigt und keine anderen als die angegebenen Hilfsmittel und Quellen benutzt habe. Ferner erkläre ich, die vorliegende Arbeit an keiner anderen Hochschule als Dissertation eingereicht zu haben. Ich habe noch keinen Promotionsversuch unternommen. Die Ergebnisse dieser Dissertation sind an den aufgeführten Stellen auszugsweise veröffentlicht.

Bonn, Datum _____ Unterschrift _____

Publikationen und Beiträge auf Fachkongressen

Publikation: N. Keksel, H. Bußmann, M. Unger, J. Drewe, G. Boonen, S. Franken, H. Häberlein. „ St John´s wort extract influences membrane fluidity and composition of phosphatidylcholine and phosphatidylethanolamine in rat C6 glioblastoma cells". Akzeptiert bei *Phytomedicine.*

Publikation: D. K. Glatzel, A. Koeberle, H. Pein, K. Loeser, A. Stark, N. Keksel, O. Werz, R. Müller, I. Bischoff, R. Fürst. „ Acetyl-CoA carboxylase 1 regulates endothelial cell migration by shifting the phospholipid composition." *Journal of Lipid Research,* 59(2), 298-311, 2018.

Vortrag: N. Keksel, H. Bußmann, M. Unger, J. Drewe, G. Boonen, S. Franken, H. Häberlein.„Influence of the St, John´s wort extract Ze117 on membrane fluidity, signal transduction, and mobility of the β-adrenergic receptor." 65. internationaler Kongress der Gesellschaft für Arzneipflanzen- und Naturstoff-Forschung e.V. (GA) in Basel, Schweiz. 2017

Poster: D. K. Glatzel, N. Keksel, A. Koeberle, O. Werz, M. Ashtikar, R. Müller, R. Fürst. „The acetyl-CoA carboxylase (ACC) inhibitor soraphen blocks the proliferation and migration of primary endothelial cells." 29. Irseer Naturstofftage der Gesellschaft für Chemische Technik und Biotechnologie e.V. (DECHEMA) in Irseer, Deutschland. 2017

Publikation: C. Greunke, A. Hage-Hülsmann, T. Sorkalla, N. Keksel, F. Häberlein , H. Häberlein. „ A systematic study on the influence of the main ingredients of an ivy leaves dry extract on the β_2-adrenergic responsiveness of human airway smooth muscle cells." *Pulmonary Pharmacology & Therapeutics*, 31, 92-98, 2015.

Danksagungen

Zuerst möchte mich ganz herzlich bei Herrn Prof. Dr. Hanns Häberlein für die Ermöglichung dieser Arbeit und die großzügigen Arbeitsbedingungen bedanken.

Darüber hinaus bedanke ich mich vielmals bei Prof. Dr. Hanns Häberlein und Dr. Sebastian Franken für die stets vorhandene Betreuung und tatkräftige Unterstützung, die wesentlich zum Gelingen dieser Arbeit beigetragen hat.

Zusätzlich möchte ich mich noch bei Dr. Sebastian Franken für die tollen Ideen bei der Entwicklung und die Unterstützung bei der Umsetzung der Massenspektrometrieanalysen bedanken. Hierbei auch meinen Dank an Dr. Marc Sylvester und Bernd Gehrig, die ebenfalls mit ihrem Know-how zur Seite standen.

Ein weiterer großer Dank geht an Herrn Prof. Dr. Christoph Thiele für die Übernahme des Koreferats und die Möglichkeit der Promotion im Fachbereich Molekulare Biomedizin. Für seine Bereitschaft, sich mehrfach mit dem Voranschreiten der Arbeit auseinanderzusetzen und dem guten Rat, die Fettsäureidentifizierung mittels anionischer PC-Addukte anzugehen, möchte ich mich ebenfalls bedanken.

Ich danke Prof. Dr. Kubitscheck und Dr. Jan-Peter Siebrasse für die Möglichkeit, die Fluoreszenzanisotropiemessungen im Institut für Physikalische und Theoretische Chemie durchzuführen zu können. Ich wurde dort freundlich aufgenommen und unterstützt.

Bei Dr. Georg Boonen, Prof. Dr. Jürgen Drewe und Dr. habil. Matthias Unger von der Max Zeller Sohne AG in Romanshorn, Schweiz, bedanke ich mich für die finanzielle Unterstützung und das große Interesse an der Thematik.

Allen Mitarbeitern der Arbeitsgruppe Häberlein danke ich für den stets freundschaftlichen Umgang und die tolle Arbeitsatmosphäre. Es war sehr lustig mit euch!